

Design and Optimization of Electrostatic MEMS Switches Using COMSOL Multiphysics: A Material Study

Asif Mirza^{a*}, Muhammad Abdul Qadeer^a, Shakeela Rasheed^b, Ashar Javed^b, Atif Hussain^a

^a Department of Physical Sciences, University of Chenab Gujrat, Pakistan.

^b Department of Physics, University of Lahore, Gujrat Campus, Gujrat, Pakistan.

Corresponding author:

Asif Mirza

Department of Physical Sciences, University of Chenab Gujrat, Pakistan.

Key Words: COMSOL Multiphysics, MEMS (Micro-Electro-Mechanical Systems), Electrostatic switches, Simulation, Material study, Design optimization

Abstract

Engineers, scientists, and researchers utilize the simulation program COMSOL Multiphysics to precisely simulate the real world and investigate a variety of physical phenomena in their models. The main purpose of this work was to study the designing and optimization of electrostatic microelectromechanical systems (MEMS) switch in COMSOL Multiphysics and the feasibility study of the electrostatic switches to come up with its higher performance, controlled actuation by using different materials. The objectives of this study are: To investigate various materials for performance of MEMS switches and to design a switch beam structure for performance. As we analyzed the results, we observed mode shapes and mode of vibrations with respect to stress analysis and Eigen frequency, displacement with respect to voltage for three different materials such as Silicon, SiN₃ and SiO₂. We observed that output parameters of Si are higher as compared to the SiN₃ and SiO₂. Si material has higher electrical and capacitive response as compared to the other two materials.

INTRODUCTION

MEMS technology incorporates mechanical components, sensors, actuators, and electronics onto a solitary silicon substrate using microfabrication methods (1-6). This technology facilitates the development of minuscule, accurate, and frequently extremely responsive devices that can detect, manipulate, and engage with their surroundings on a microscale. MEMS devices are extensively utilized in a diverse range of applications, including accelerometers, gyroscopes, pressure sensors, microphones, inkjet printers, and biomedical equipment. They have benefits such as compactness, minimal energy usage, exceptional dependability, and affordability, rendering them indispensable elements in contemporary electronics and engineering systems (1, 2).

MEMS electrostatic switches are compact devices that utilize electrostatic forces to manipulate the motion of mechanical components (7). These switches are frequently employed in situations where rapid reaction, minimal power usage, and compact size are crucial. The fundamental working principle of an electrostatic MEMS switch is based on the interplay of electrostatic forces between stationary and mobile electrodes. Here is the operational process: The switch is composed of a mobile electrode, also referred to as a beam, and a stationary electrode. The mobile electrode is linked to the mobile contact, which forms a component of the switching mechanism. Electrostatic actuation occurs when a voltage is arranged between the fixed and movable electrodes, resulting in the creation of electrostatic forces (7). The movable electrode is influenced by these forces, causing it to either move closer to or further away from the fixed electrode. The direction of movement is determined by the polarity of the supplied voltage. When the switch is in the "off" state, the moveable electrode is positioned at a distance from the fixed electrode, creating an air gap between them. When an external signal, such as a control voltage, is applied, the movable electrode is attracted towards the fixed electrode by the electrostatic force. When the movable electrode touches the fixed electrode, the switch changes to the "on" state. On the other hand, if the control voltage is removed, the movable electrode will go back to its initial position, causing the contact to break and switching the switch to the "off" state (1, 2, 8).

The MEMS based switches have the ability of rapid response time facilitated by the electrostatic actuation system. The structure and driving manners are straightforward and uncomplicated and minimal energy consumption. The switches can be utilized in aerospace, communication, test and measurement, and automatic control industries. Superior signal switching quality due to physical contact and separation, distinguishing them from electronic switches.

Electrostatic drive is a well-established and extensively studied driving principle in the field of MEMS. Other drive concepts encompass electromagnetic, piezoelectric, and electro-thermal approaches. Each approach possesses unique benefits and drawbacks, but, electrostatic MEMS switches continue to be favored for their straightforwardness and effectiveness (1, 2).

The mechanical movement of the switch is achieved by utilizing electrostatic, magneto statics, piezoelectric or thermal designs (5). In existing industry, electrostatic switches have greater consistency and large frequencies. Magneto statics actuation demands high voltages and has low switching speeds, relatively high-power consumption. Thermal actuators also require high voltages and have low switching speeds and again, they display greater power utilization. In short, electrostatic actuation is the ideal category for MEMS switches. It also has high switching speeds along with less power consumption. Electrostatic MEMS switches also have greater reliability so finding a comparatively suitable material for switches is very important (4-6, 9).

RESEARCH METHODOLOGY

COMSOL Multiphysics which is a finite element analysis (FEA) based software is used to design and simulate MEMS based electrostatic switches and other devices (1-3, 10-14). COMSOL Multiphysics is essential for simulating Microelectromechanical Systems (MEMS), especially for electrostatic switches. The MEMS Module in COMSOL Multiphysics offers specialised features designed for modelling MEMS devices. Users can use it to estimate the structural, electrical, and thermal performance of MEMS devices correctly and efficiently. This module facilitates comprehensive simulations of electrostatic switches, allowing for precise analysis of their behaviour, encompassing capacitance variations, contact pressures, and response durations (15). A radio frequency (RF) MEMS switch is an electromechanical device frequently encountered in RF systems. These switches function at radio frequency (RF) frequencies, demonstrate significant isolation (minimum power loss while deactivated), low insertion loss (little signal power loss when activated), and exceptionally low power consumption. Engineers may effectively simulate RF MEMS switches using COMSOL Multiphysics. An instance of this is the RF MEMS Switch model found in the COMSOL Model Gallery, which showcases the analysis of contact forces and variations in capacitance that occur during the operation of the switch. Engineers obtain vital insights into switch behaviour by estimating the time it takes for the bridge to come into contact with the film and calculating the capacitance after the bridge is completely drawn in. Improving

COMSOL improves comprehension, minimises the need for physical prototypes, and facilitates superior product development (14).

Figure 1 describes the procedure and method to achieve the objectives of proposed work. Modeling and simulation will be performed using COMSOL tool. Design parameters will be selected within micro scale range. Boundary conditions will be applied for behavioral analysis.

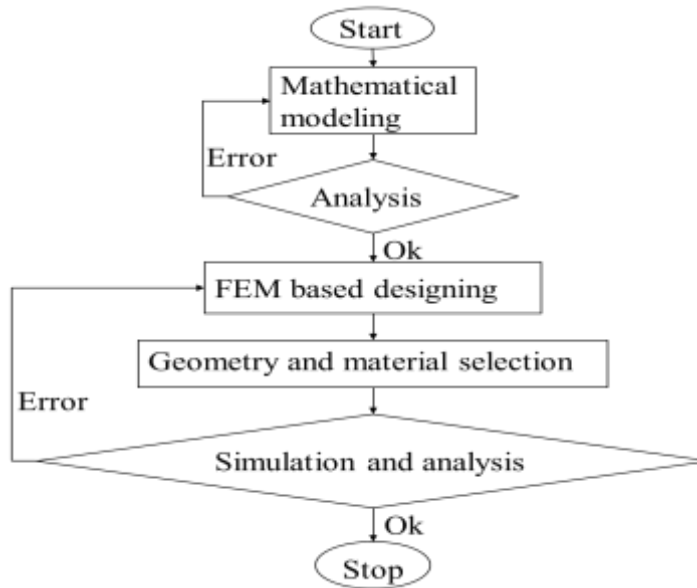
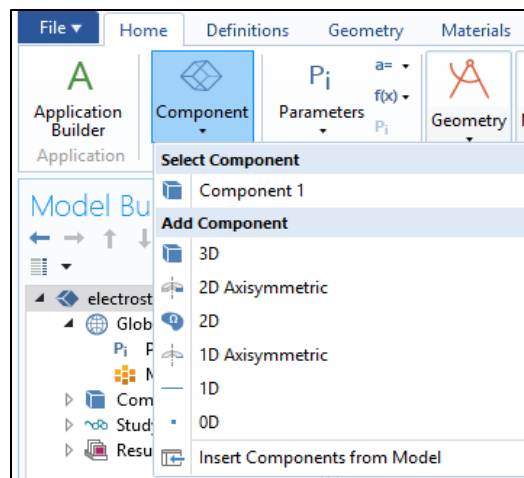


Figure 1. Basic Framework

The following steps have been taken to develop proposed design of MEMS switch. From the GUI window we chose the command ‘Add Component’ then 3D command is selected for designing of proposed device (Fig.2).

Figure 2. Selection of design model



Then physics is added in the model for any kind of analysis in electrical, mechanical, optical, and chemical domain (Fig. 3).

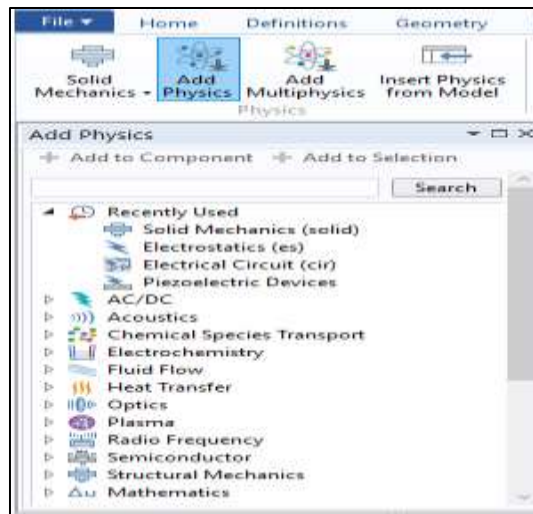


Figure 3. Selection of physics type for model analysis

In the last a study is added by using command 'Add Study' for FEM based simulation of designed model (Fig.4). The model can be observed and investigated using eigenfrequency, frequency domain, stationery, and time dependent analysis.

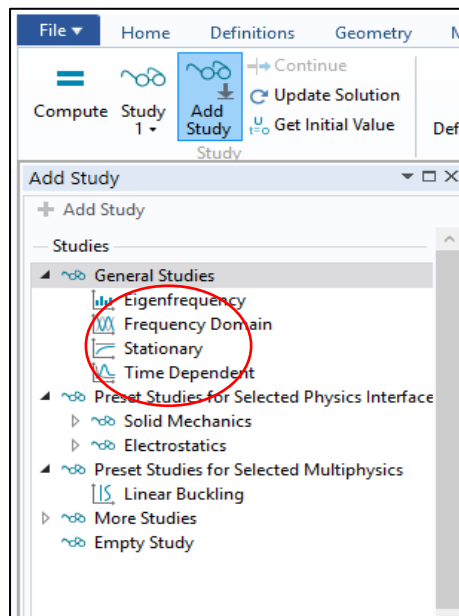


Figure 4. Selection of study type for the model analysis

First, we designed geometry of the MEMS switch structure. In geometry window micrometer was selected from Length unit dropdown list as shown in Figure 5. Then structure of the switch is developed by choosing 3D blocks in geometry section provided in the model builder window.

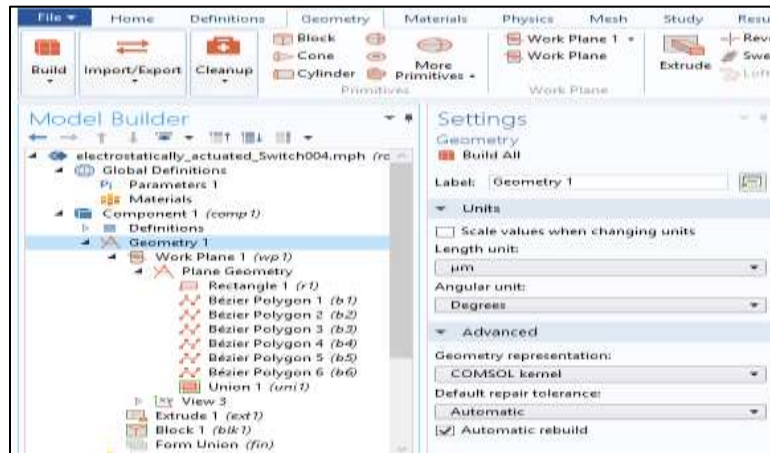


Figure 5. Geometry of model structure

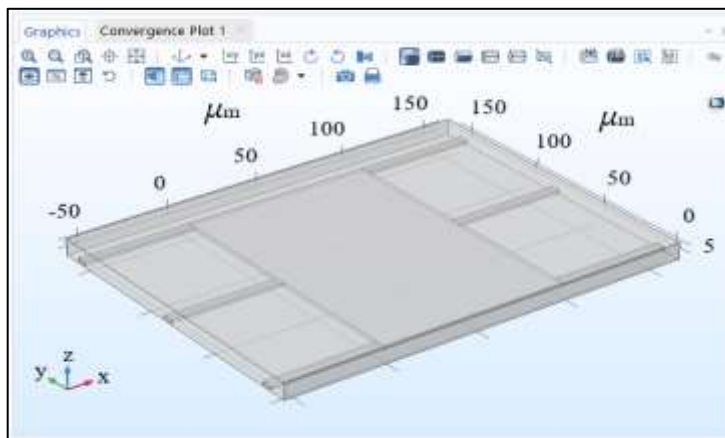


Figure 6. 3D structure of switch

After completion of the switch model different materials are added for air box and switch. The materials are added by selecting the command of add material from home menu or right clicking on materials nod in the model builder window as displayed in figure 7 and 8.

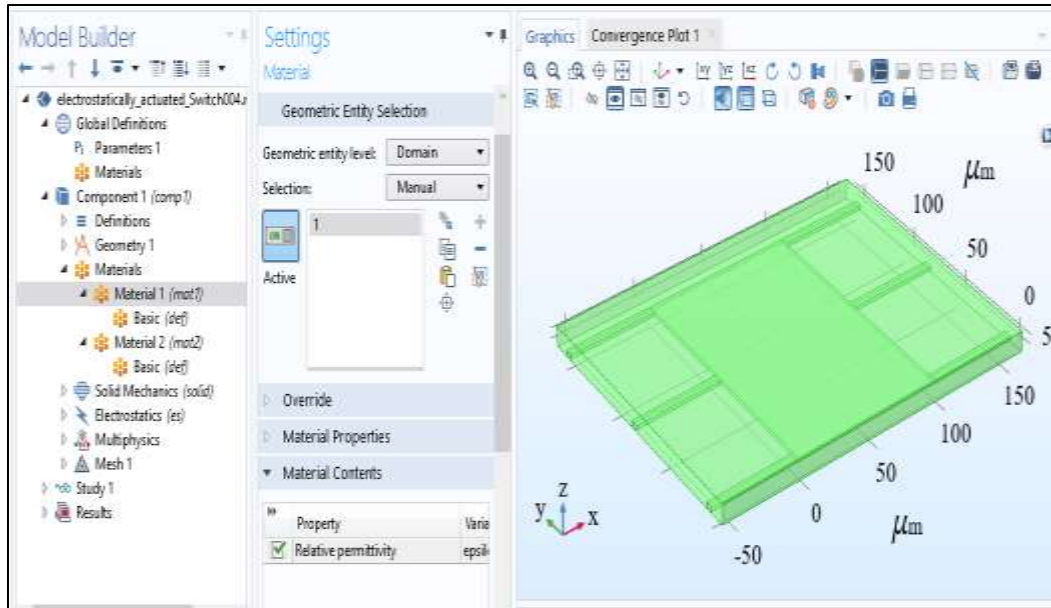


Figure 7. Assigning air to the box model

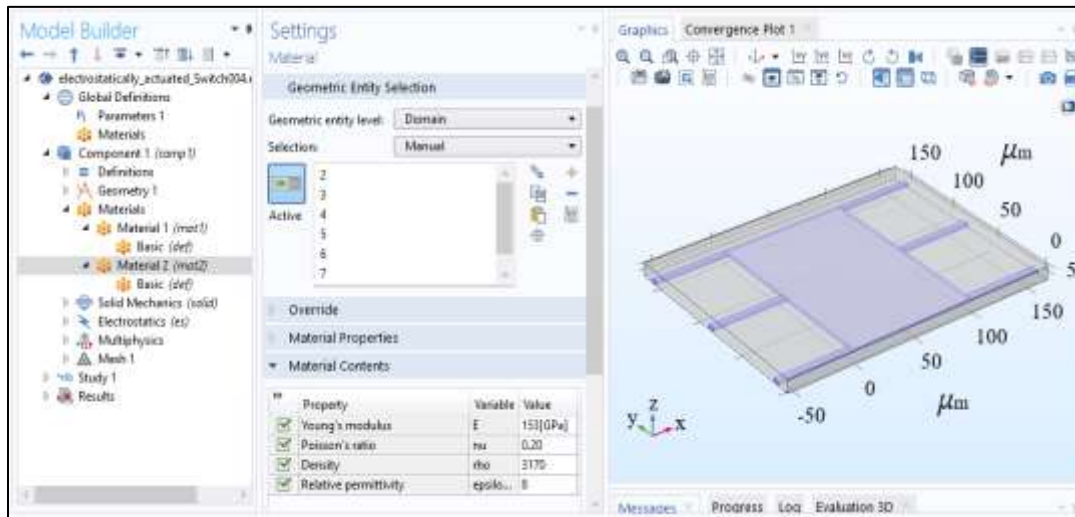


Figure 8. Assigning materials to the structure of switch

Figure 9 shows the two modules of physics i.e. solid mechanics (solid) and electrostatic (es).

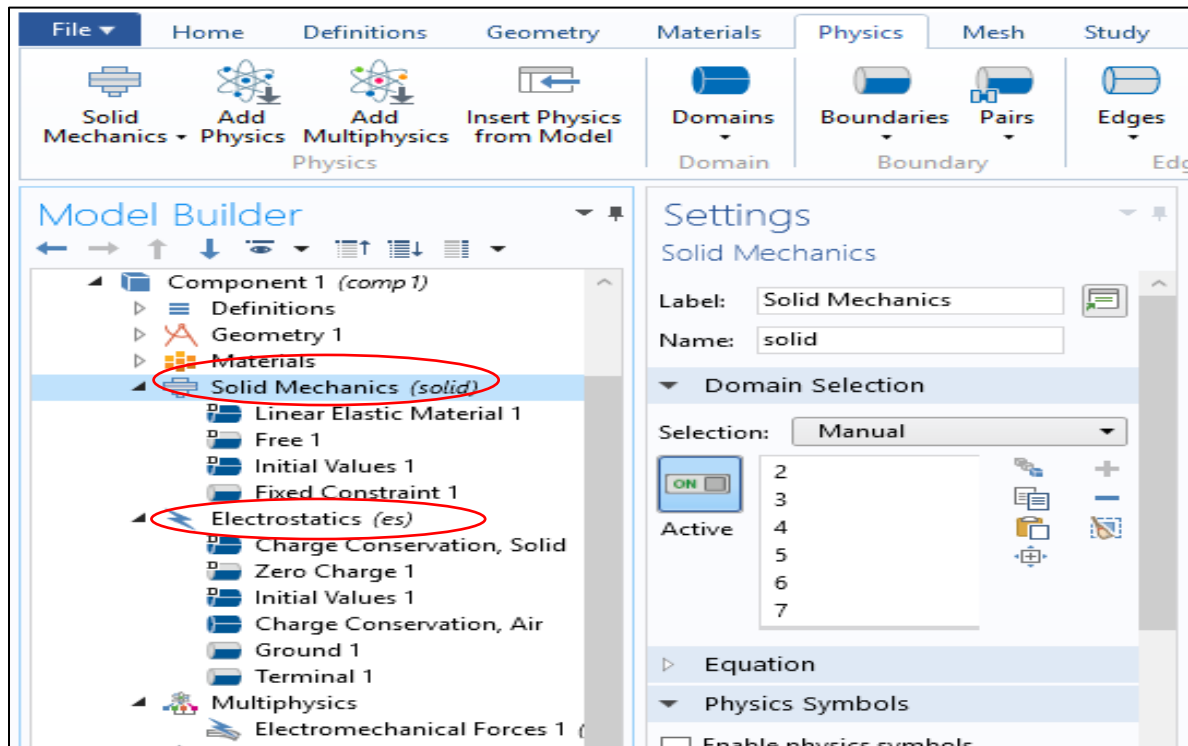


Figure 9. Assigning physics module

There are three boundary comodule...ns namely fixed constraints terminal and ground. In the setting window of physics modules boundary conditions are applied by selecting domains. In the model builder window fixed contain is used to fix any part of the structure. In the setting window, the six beams of the structure are fixed by selecting six faces in the boundary selection menu. In the selection menu the numbers 5, 10, 15, 48, 49 and 50 represent the six faces highlighted in blue color in the graphic window as revealed in Figure 10.

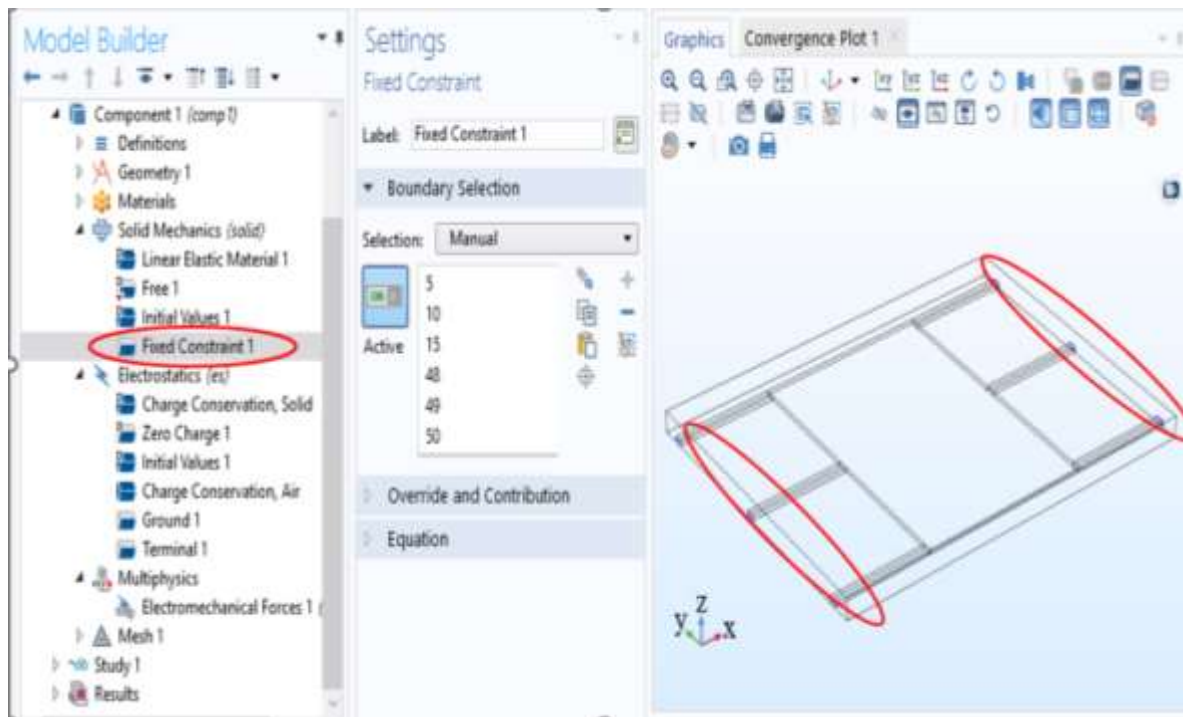


Figure 10 . Selection of boundary for applying fixed constraint

Figure 11 displays the setting window of terminal for applying voltage. When a specific area of electrical contact is selected shown in red circle, a boundary number 3 is appeared in the selection menu which shows the ground plate of the capacitor.

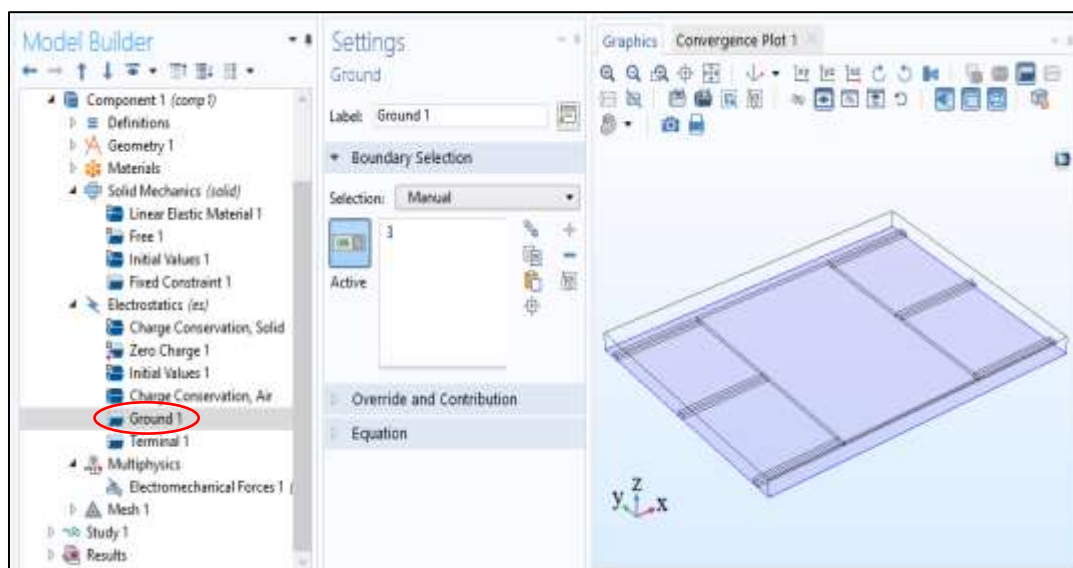


Figure 11. Selection of boundary for applying ground

Figure 12 represents the boundary of terminal voltage. In the terminal setting window six boundaries are selected for applying terminal biased voltage. Then voltage value is added in the dropdown list of terminal type.

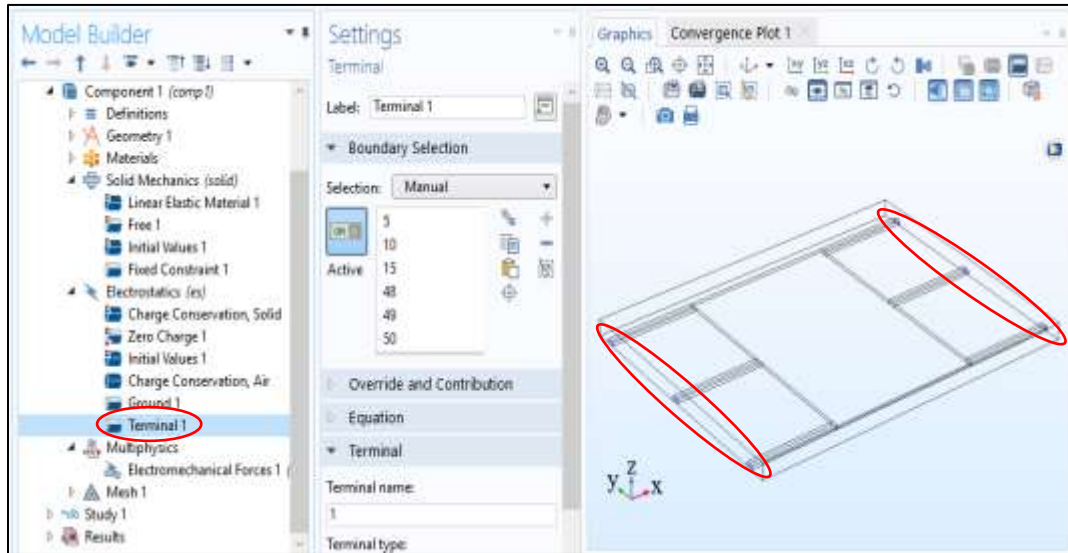


Figure 12. Selection of boundary for applying ground potential

Meshing of Device Model

Figure 13 shows the meshing window; in the setting we can change the mesh size and element type. Meshing is performed by selecting 'domain' from geometric entity level and 'all domains' in selection list. The model is ready for meshing after applying boundary conditions. Free tetrahedral is selected from mesh menu. Then meshing is performed by choosing the option 'build all' as shown in figure 13. Finally, the command 'build all' is selected to perform meshing. After successful meshing, model is ready for simulation.

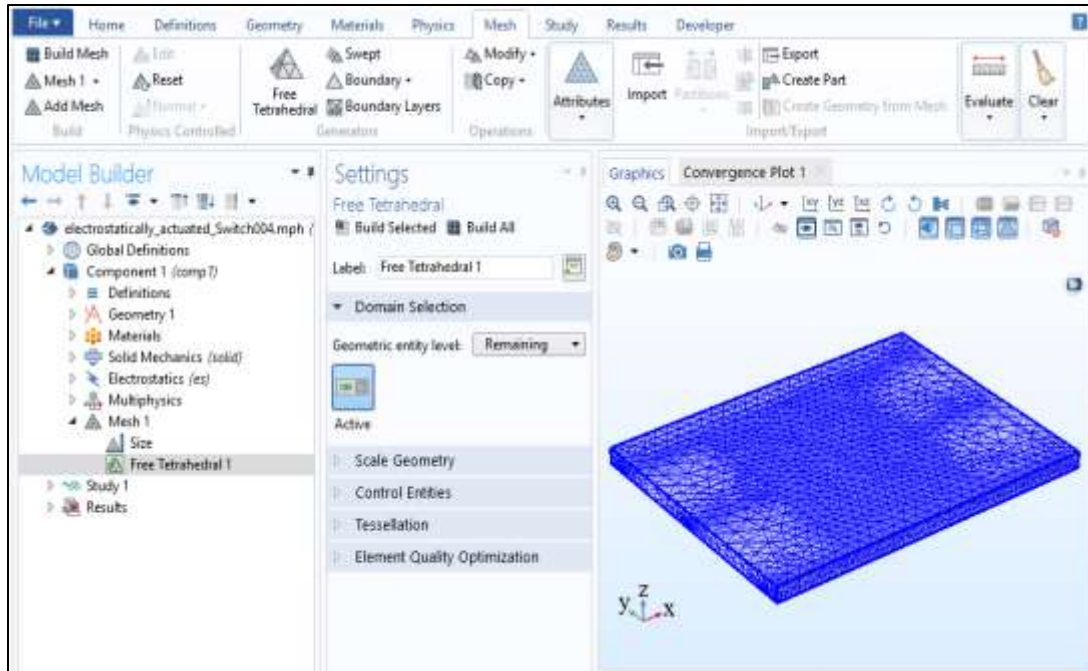


Figure 13 Meshing the model of proposed device

In the model builder setting window is open by clicking on the study. Then simulation is performed by pressing the compute button shown in figure 14. In the setting window, we used the auxiliary sweep with respect to biased voltage. We added voltage range from 1V-10V by selecting the option range indicated by red circle.

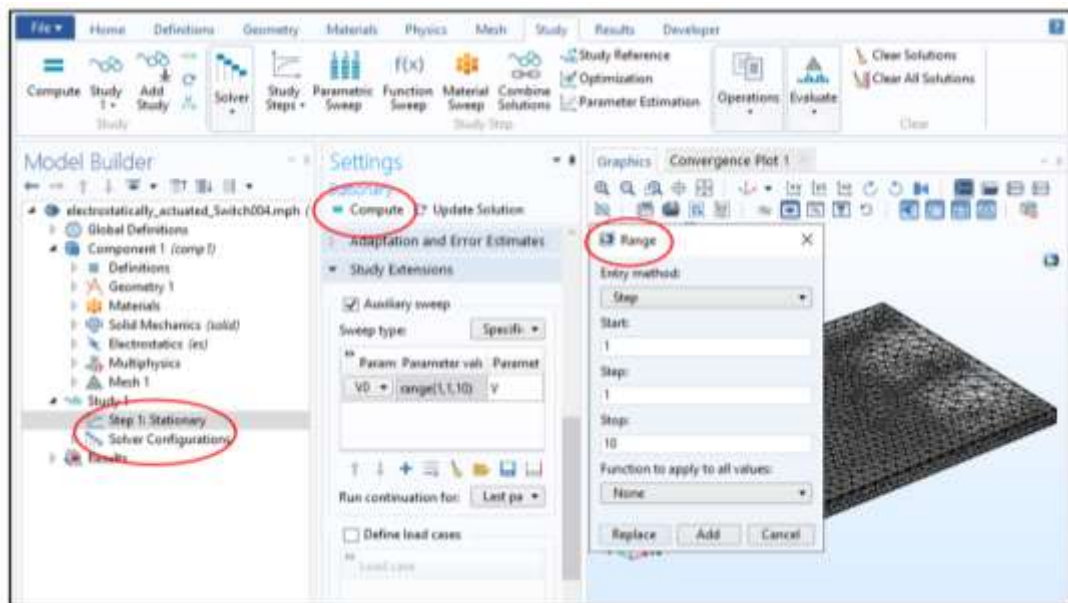


Figure 14. Computing the model after meshing

Plotting Graphs

The default results of the model are displayed after computation. Simulation generates the 3D graphs of vertical displacement and electric potential as shown in figure15. Other parameters can be plotted by selecting differing graphs upon right clicking on the node of results. We can also plot 1D graphs of 3D structure. Figure 16 shows the scheme of line graph between applied voltages and displacement. 1D plot is obtained by clicking on the 1D plot group available in the quick access bar of Results menu. I appear in the tree nodes of results shown in model builder window. Then we choose line graph by clicking right on the 1D plot group. We go to selection menu in the window of line graph setting. We switch it on to activate the boundaries of the model. We selected three adjacent lines of the model in graphic window indicated by red circle. We noticed that three boundaries 8, 35, 55 appeared in the selection menu. Finally, the graph is drawn by clicking on the plot button in the window of line graph settings.

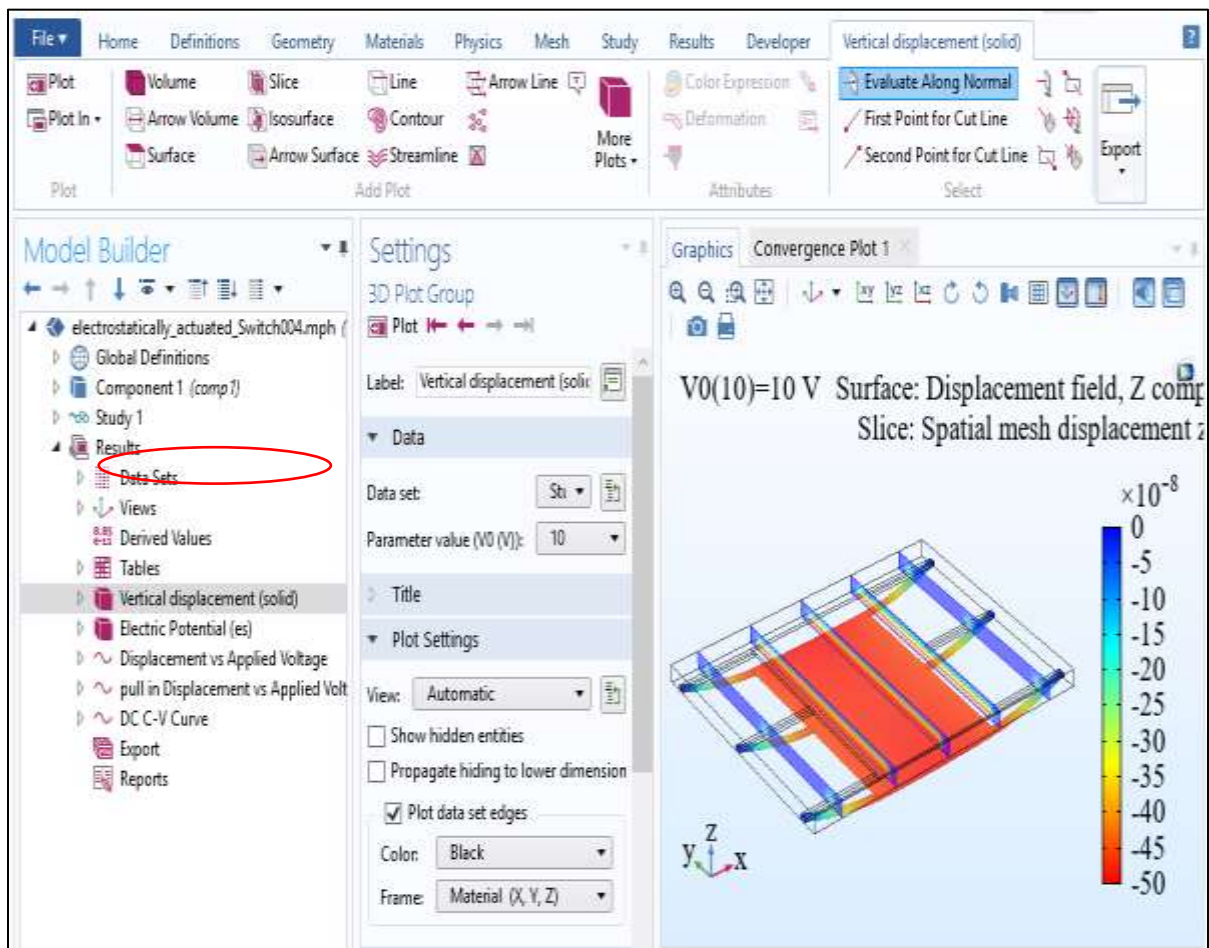


Figure 15. Default result of proposed model after simulation

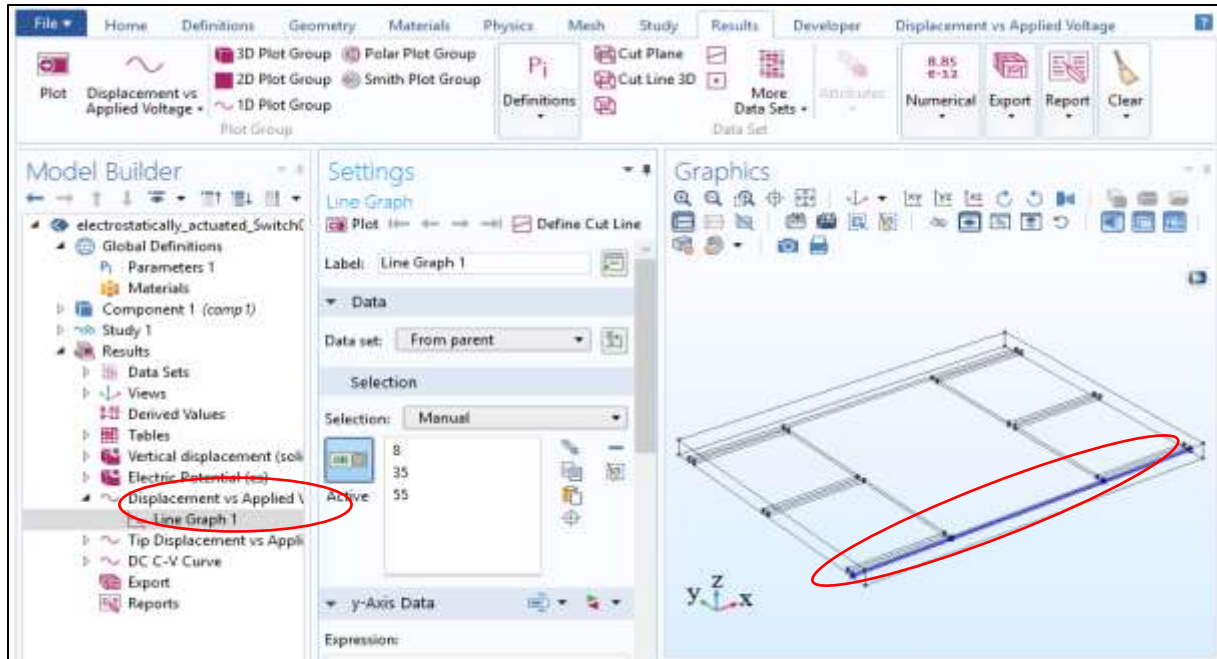


Figure 16. Plotting line graph of proposed model after simulation

RESULTS AND DISCUSSION

This part of the paper discusses the outputs of this study of single crystal Silicon (Si), Silicon Dioxide (SiO_2) and Silicon Nitride (SiN_3) based MEMS Switches. This part starts with Section 1 which presents the details of device design including material, geometry, and meshing. Section 2 describes the structural analysis, in terms of Eigen frequency, modes of vibrations and stresses of structure of switch. Section3 presents the performance analysis of the Si based device with respect to biased voltage, electrical potential and change in capacitance. Sections 4and 5 describes the results of performance parameters of SiO_2 and SiN_3 based devices. In the last section 6 presents the comparison of performance parameters of all three proposed devices.

Dimension and Material Properties of Electrostatic Switch

This model investigates a MEMS switch containing a suspended thin micromechanical plate above a dielectric layer. When a DC voltage larger than the pull-in voltage connected to the switch, it leads to the plate collapsing on the dielectric layer which causes an enhancement in the capacitance of the device. To model the contact forces a compensation, contact force is instigated as the plate is come into contact with the dielectric layer. For handling both conducting and dielectric materials we demonstrated the ability of the electro mechanics multi physics interface.

The device geometry is displayed in Figure 17. The switch contains a square plate hanging $1\ \mu\text{m}$ above the ground electrode of air box having dielectric constant 2.5. We considered surface of air box below the plate as ground electrode. The suspended plate is kept electrically isolated from the substrate. Six rectangular flexures were used to anchor the suspended plate with the substrate. The designing and simulation of proposed model is performed by using COMSOL Multi physics software. The designing and material parameters are given in tables 1 and 2. Solid mechanics and electro mechanics modules were used for finite element modeling of the device. The stationary solver was used from the study tree for analysis of the device. We used three types of materials Si, SiO_2 and SiN_3 for electrostatic application. Table 2 depicts the qualities of all three materials. In COMSOL, we used geometry module for 3D designing of the device. Global axes were used for orientation of the structure. Tables 1 and 2 show both material range and geometric range of the devices. The expected results are produced by applying the proper boundary conditions to the model. Boundary conditions used for our model are the fixed constraints and biased voltage.

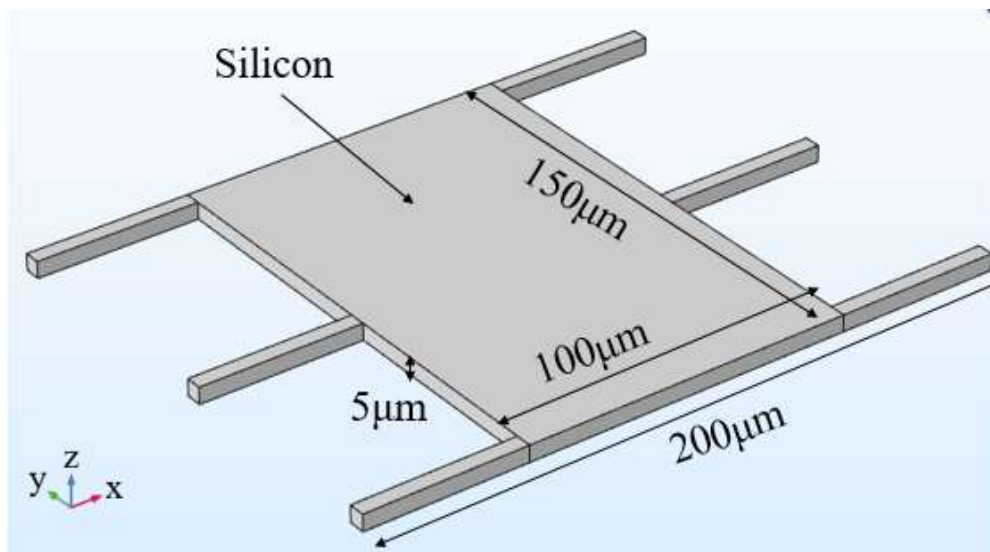


Figure 17. Structural Design of membrane based electrostatic switch

Table 1. Geometric and material parameters of pressure sensor

Parameters	Dimensions
Length of membrane	150 μm
Width of membrane	100 μm
Height of membrane	5 μm
Length of beam	50 μm
Width of beam	5 μm
Height of beam	5 μm

COMSOL is used for designing and meshing of model. Normal mesh settings of free tetrahedral are used for device structure as shown in Figure 18. Meshing procedure is one of the key processes for FEM analysis. Particularly in this work, it is essential to set up a proper and effective meshing. In case of simple geometries, the default setting can be used in COMSOL, and good results can be produced without fine meshing. For convergence simulation, the meshing was refined which caused in increasing computational time. However, the computational time was reduced by selecting the specific regions of model and meshing was redefined for those parts. Conversely the coarse meshing for the model can severely affect the results. Obviously, convergence study must be performed in both cases, but it is essential to decide for the dense mesh in advance. Certainly, it will help in speeding up the simulations.

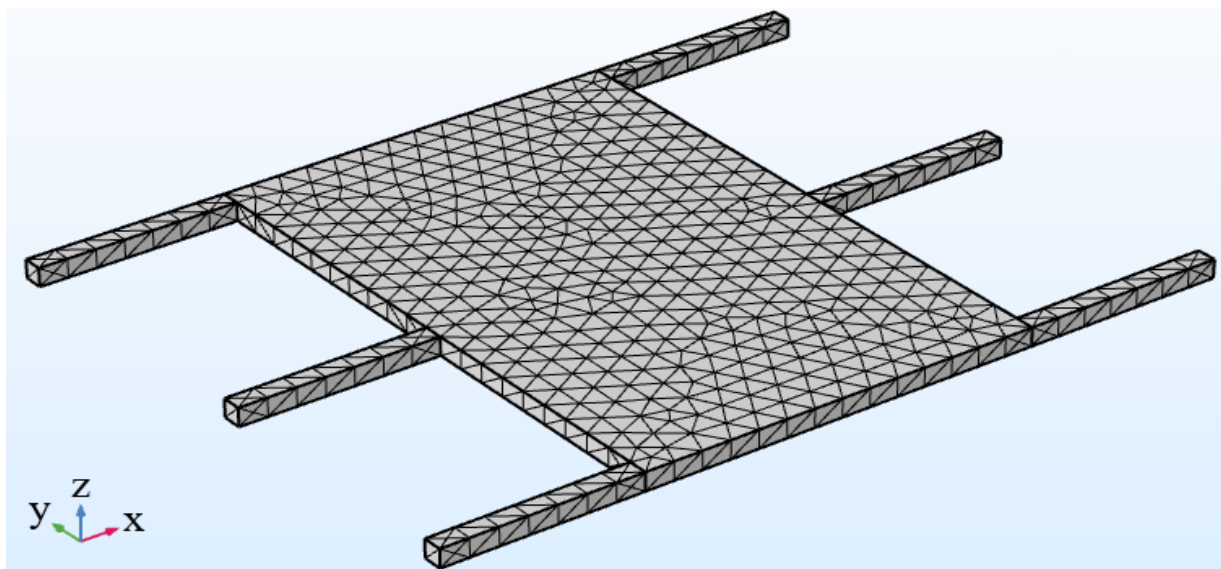


Figure 18. Meshing of proposed device model**Table 2.** Properties of different materials used in the device structure

Material Properties	Si	SiN₃	SiO₂
Young's modulus (GPa)	170	153	74.8
Poisson ratio	0.28	0.20	0.19
Density (kg/m ³)	2329	3170	2170
Relative permittivity	11.7	8	3.9

Analysis of Mode Shapes and Stresses in the Si Switch Structure

This section investigates the behavior of devices in terms of modes and stresses. The dynamic characteristics of devices are intensely depending on electric and mechanical elements, material properties and their geometry. There is mutual relation among electric and mechanical dynamics in the device. Therefore, for virtual prototyping, finite element modeling and simulation is considered as more efficient designing approach for electrostatic devices. Table 3. shows six different modes of vibration under Eigen frequencies. The change in Eigen frequency caused a change in mode shape.

Table 3. Eigen frequency and mode shapes of MEMS based switch

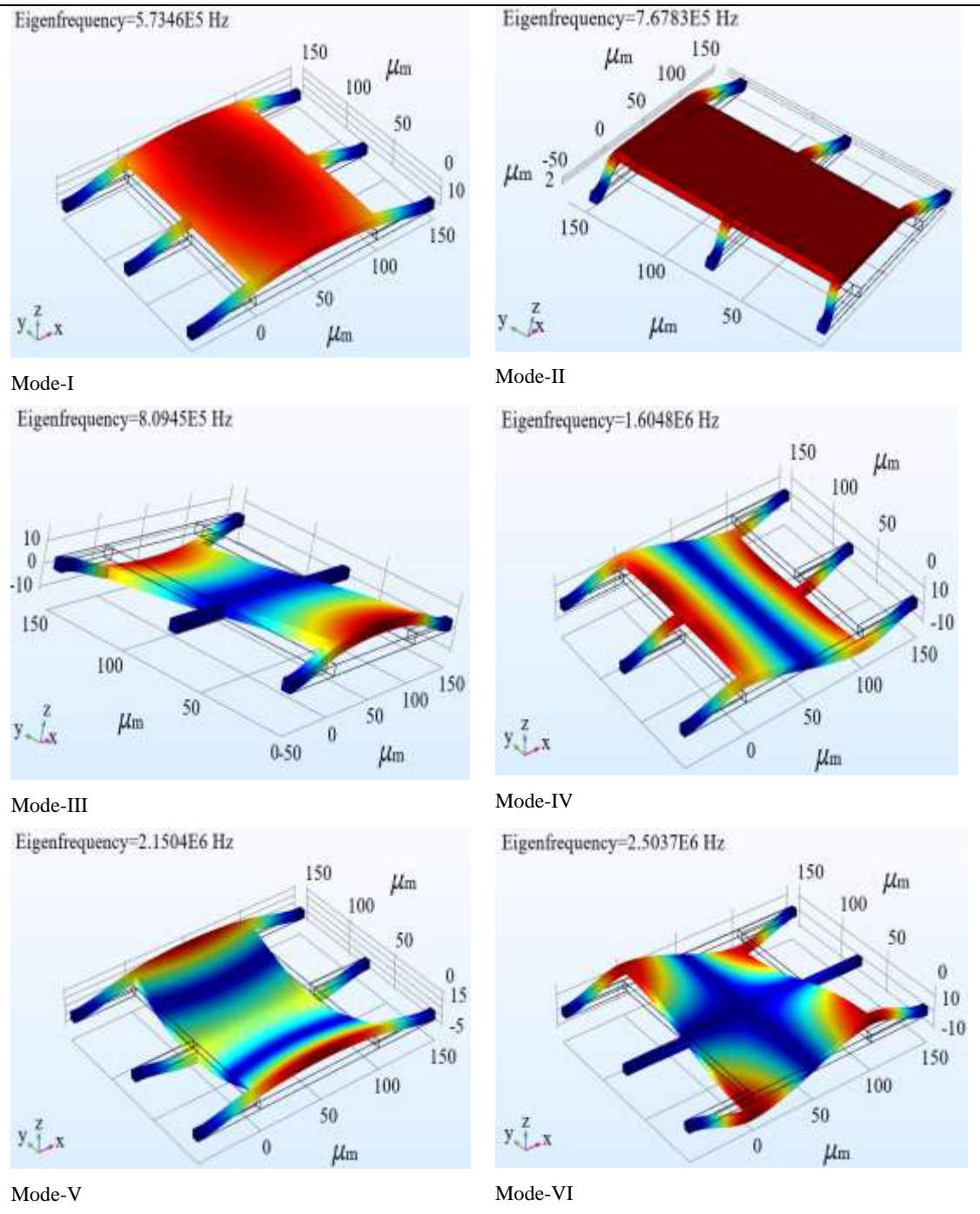


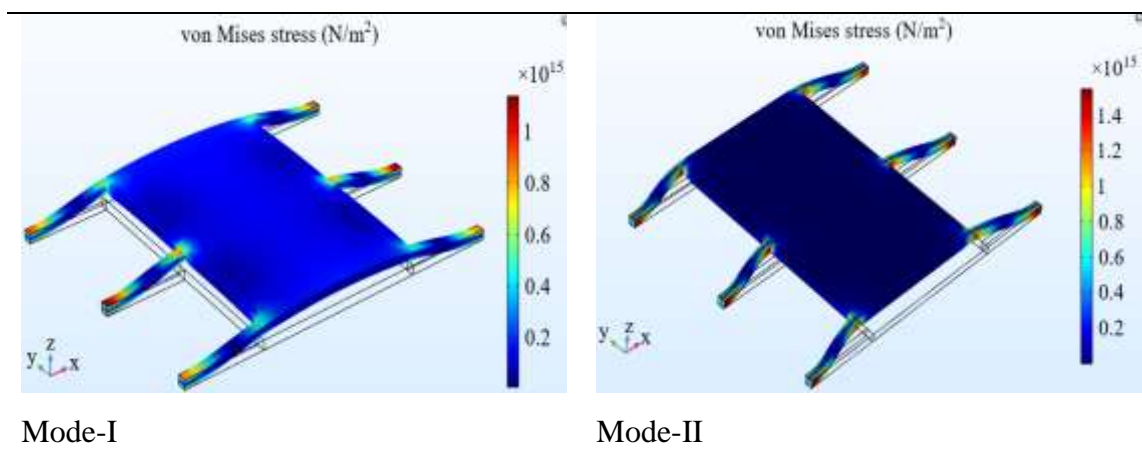
Table 4. shows the stress distribution and different modes of vibrations. For stress analysis we used linear elastic, homogeneous and isotropic properties of the materials. We considered three dimensional problems by applying the conditions of elastic -stretching and compression in

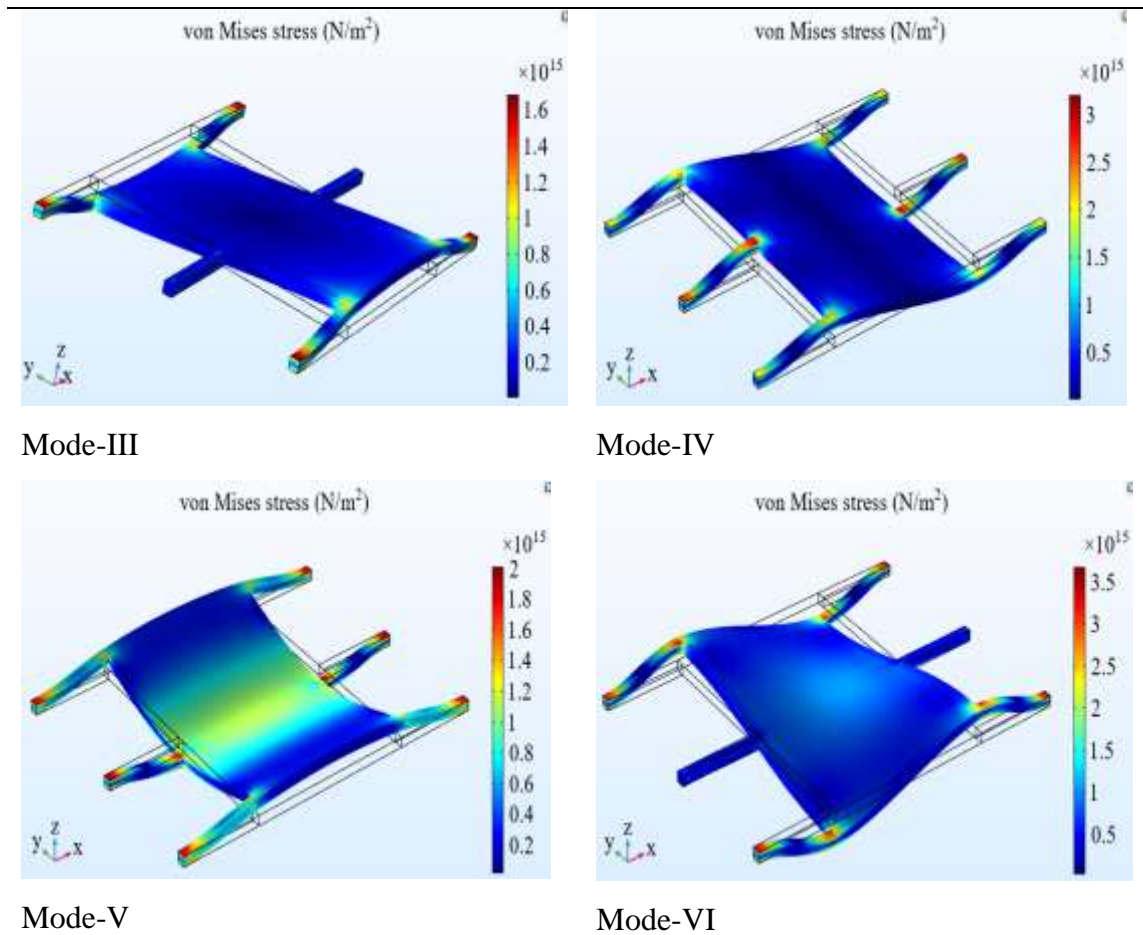
perpendicular directions for the displacement of structure. We applied boundary conditions for the approximate solution of the device was obtained from the general set of simulations. The values of stress and displacement were calculated by using a particular set of simulations.

Color bars denotes the lesser and greater values of stresses created in the device. Von Mises stress is a charge used to define material yield or failure. This study is generally used for alloys and ductile materials, for example metals. The von Mises surrenders standard condition that if the von Mises stress of a material below load is alike or bigger than the capitulate border of the equivalent material under plain strain, then the material will yield.

The membrane under loading effect is displaced due to stress-strain relation. The stress is produced due to external force and membrane is displaced due to deformation produced by the strain. This relation represents the property of the material that composes the body. The stress produced in mode-I is 3.8×10^{13} N/m², while in mode-II is 1.8×10^{12} N/m². In mode-III stress raises a little bit higher, however in mode-IV the stress was increased up to 1.4×10^{13} N/m². The mode-V shows lower value of stress which is 7.5×10^{12} N/m², while the stress value is increased in mode-VI which is 1.8×10^{13} N/m².

Table 4. Stress distribution in the structure of switch with respect to six modes





Performance Analysis of Si Based Switch

The deformation in the structure of the device is directly associated with the electrostatic forces. The forces push the plate towards the grounded substrate causes a reduction in the air gap. Consequently, this activity increases the stress forces. The stress forces are overcome by the electrostatic forces generated at a definite voltage, which causes gap collapsing due to instability of the system. This critical voltage is called the pull-in voltage. Therefore, applied voltage should be lesser than the pull-in voltage so that the plate should maintain the equilibrium position by balancing the electrostatic and forces of stress. Figure 19. depicts the displacement of the plate and consequent displacement of the surrounding mesh. Figure 20. displays the electric potential and electric field that produces these displacements.

Figure 19. Displacement of membrane with respect to voltage

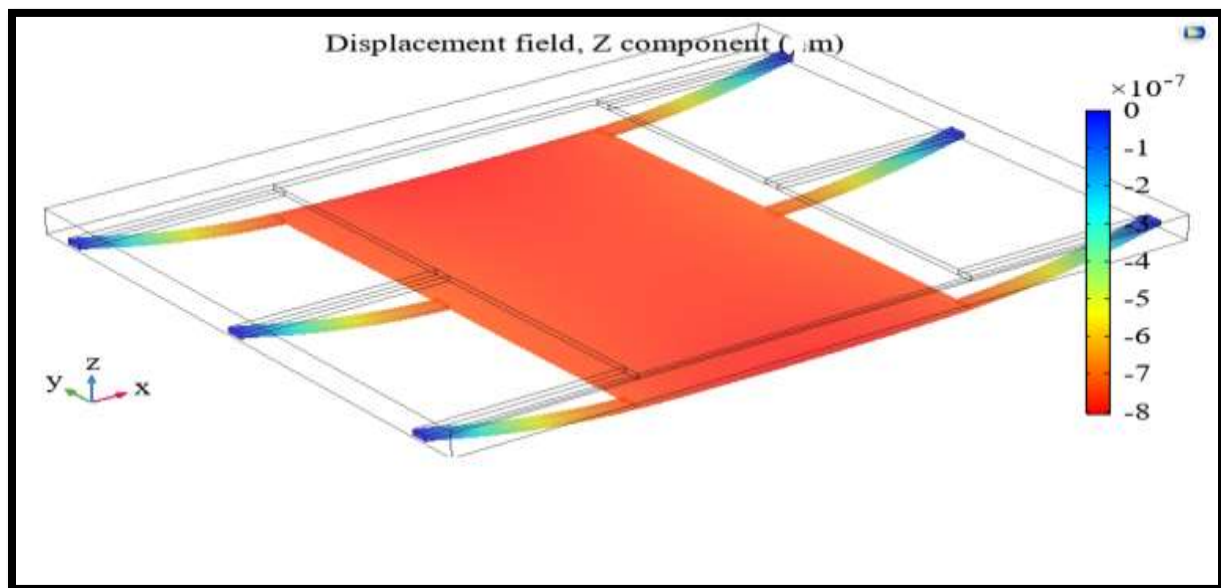
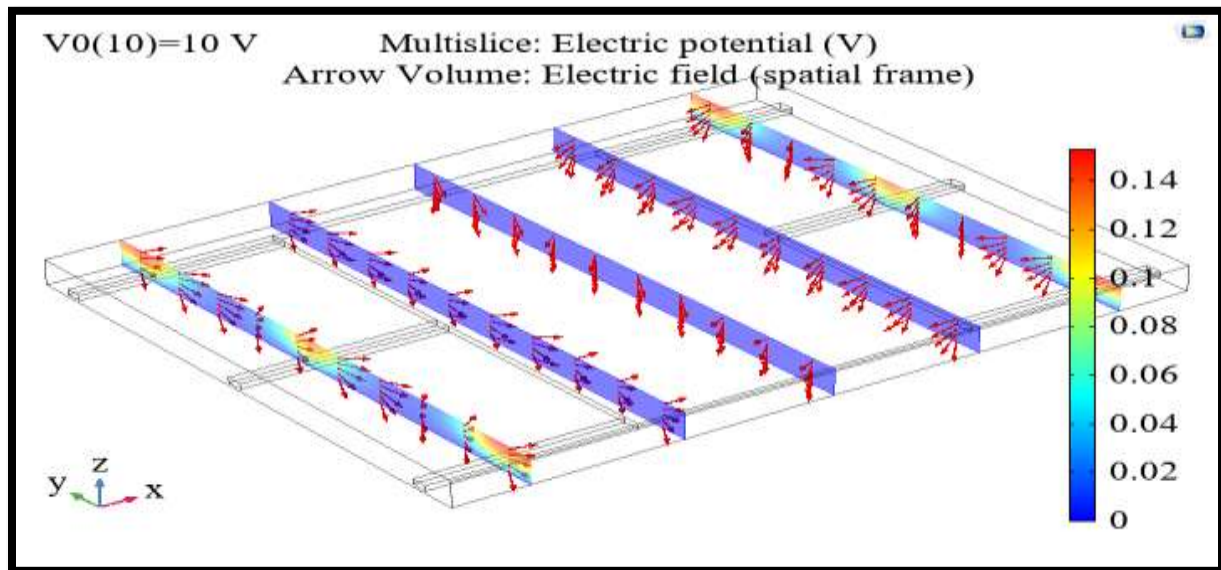


Figure. 20 Electric field and electric potential

Figure 21. displays the character of the cantilever's deflection for each useful voltage, the symmetry boundary is used by to plot the z-displacement underneath the device plate. The line graph in figure 22. illustrates the deflection as an occupation of applied voltage. We noticed that the solution does not converge when the applied voltage is increased more than the pull-in voltage. This condition takes place when the applied voltage increased up to 10V. The pull-in voltage is as a result among 9 V and 10 V.

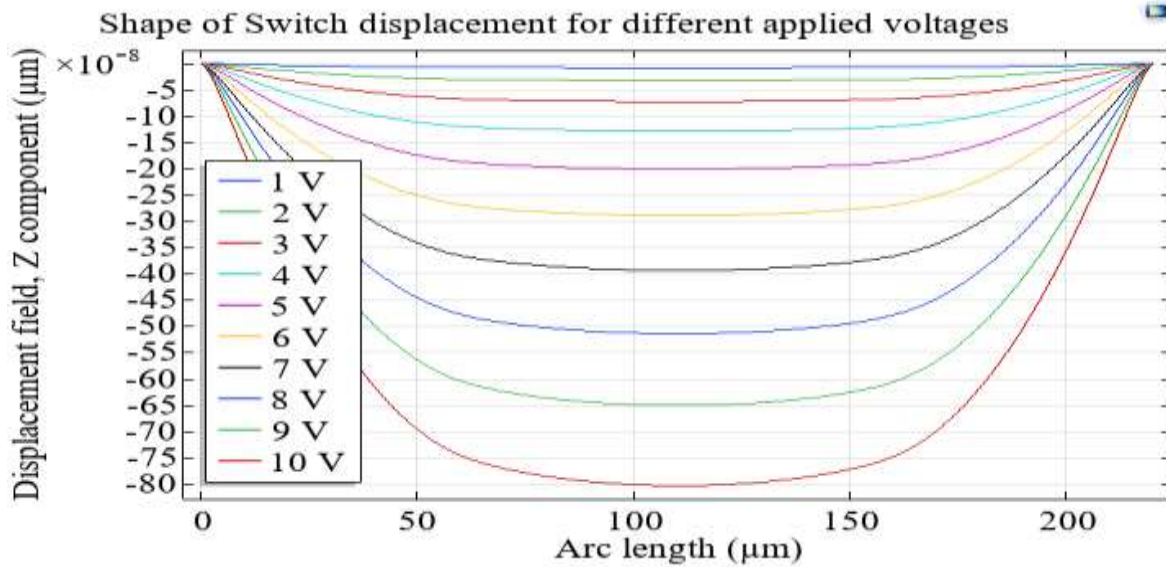


Figure 21. Change in shape of displacement due to biased voltage

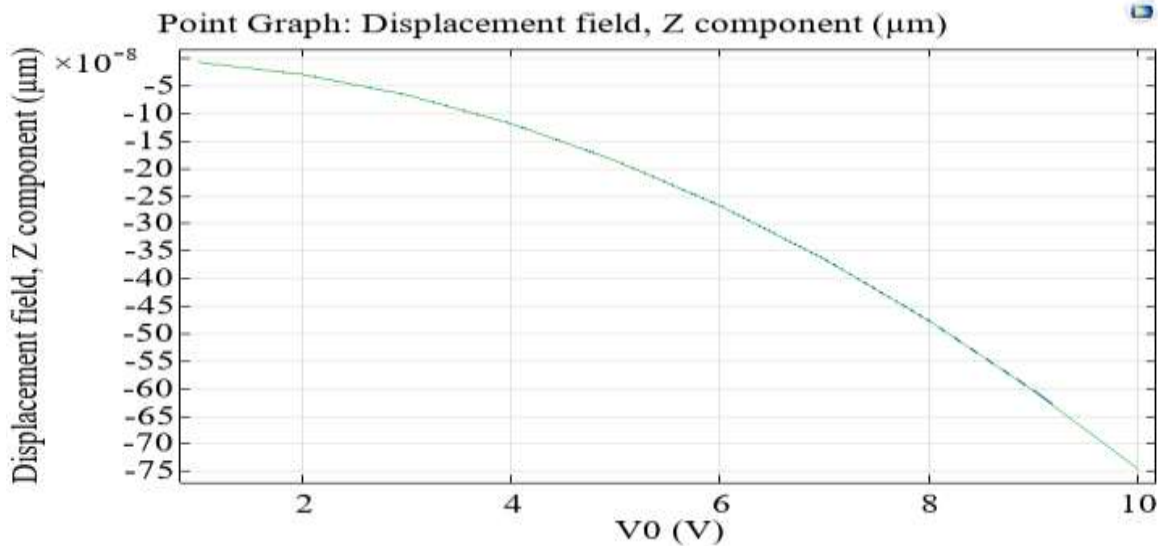


Figure 22. Change in shape of displacement due to biased voltage

Figure 23. predicts the capacitance of the device through the DC C-V curve. This analysis is like the behavior of parallel plate capacitor, whose capacitance rises with falling air gap among the plates. However, this step does not explain the overall observed capacitance due to applied voltage. The gradual softening of the coupled electromechanical system also contributes in increasing capacitance.

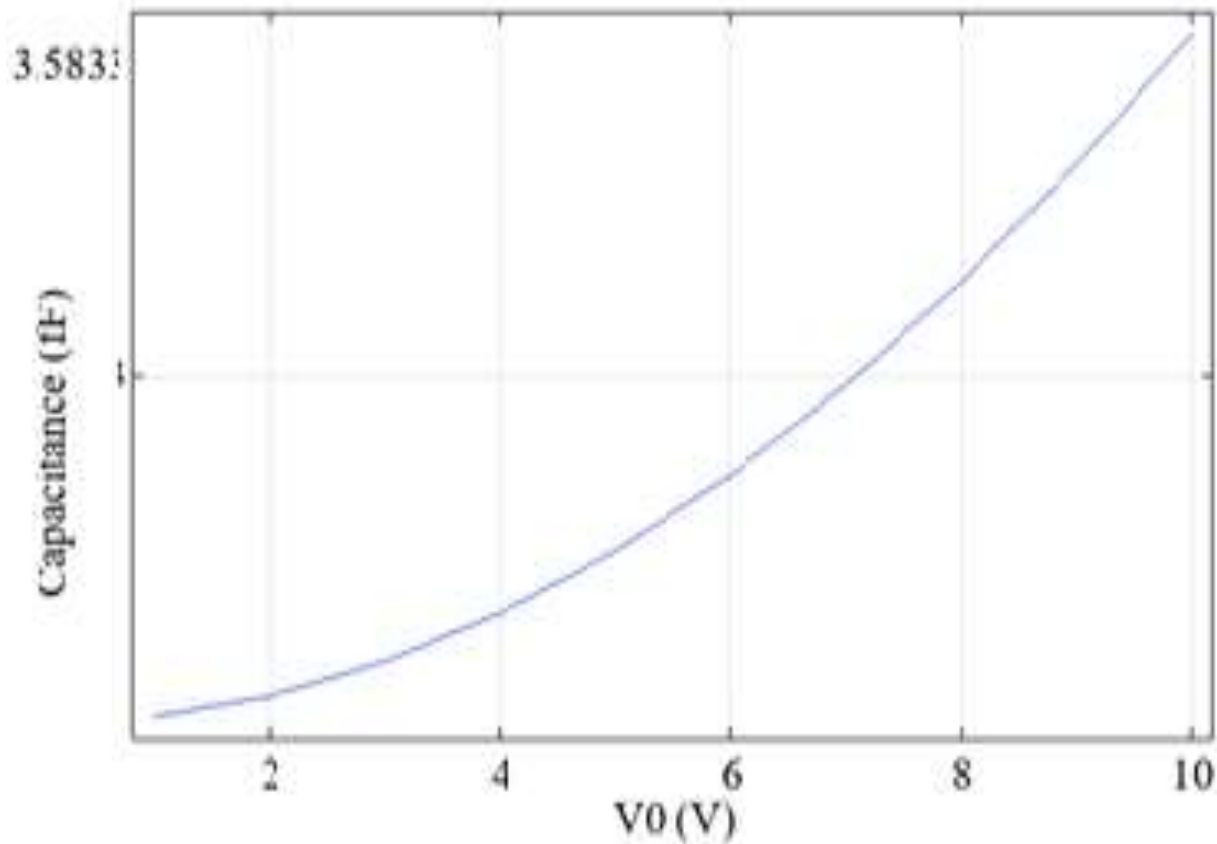
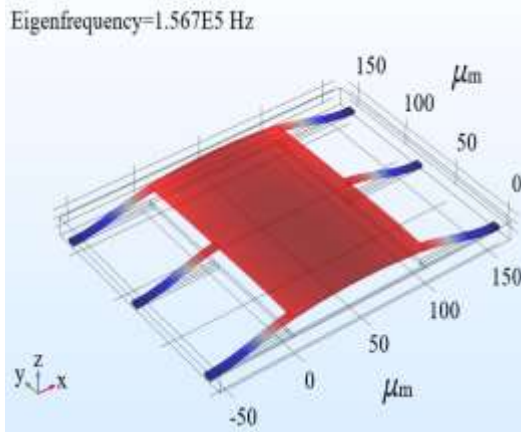


Figure 22. Effect of biased voltage on the capacitance

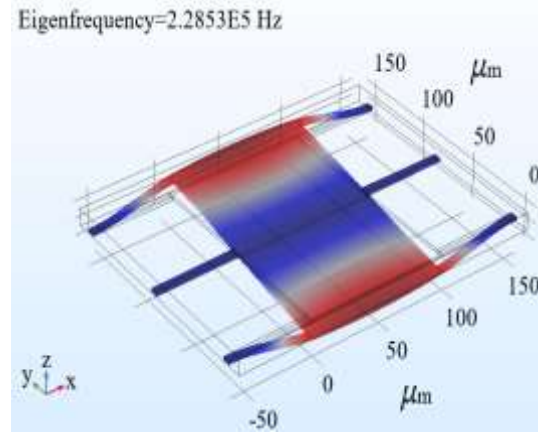
Performance Analysis of SiN₃ Based Switch

This section also investigates the behavior of device in terms of modes and stresses. The dynamic characteristics of devices are intensely depending on electric and mechanical elements, material properties and their geometry. There is mutual relation among electric and mechanical dynamics in the device. Therefore, for virtual prototyping, finite element modeling and simulation is considered as more efficient designing approach for electrostatic devices.

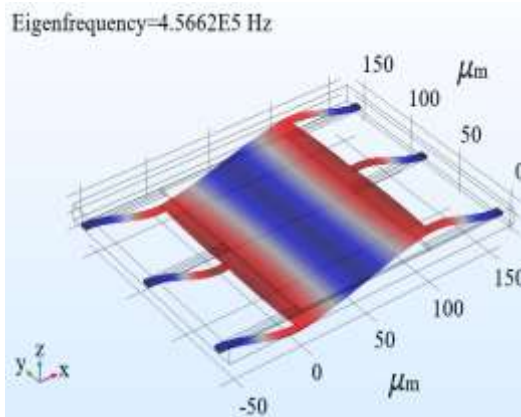
Table 5. Eigen frequency and mode shapes of MEMS based switch



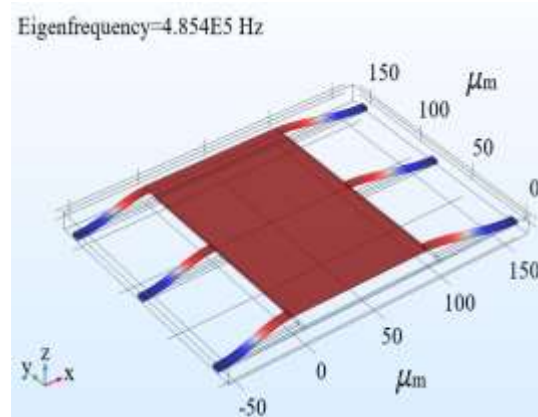
Mode-I



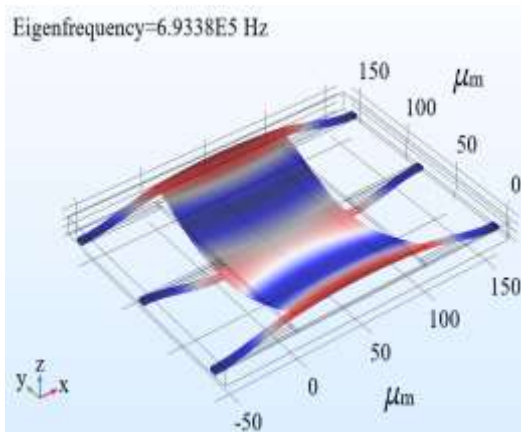
Mode-II



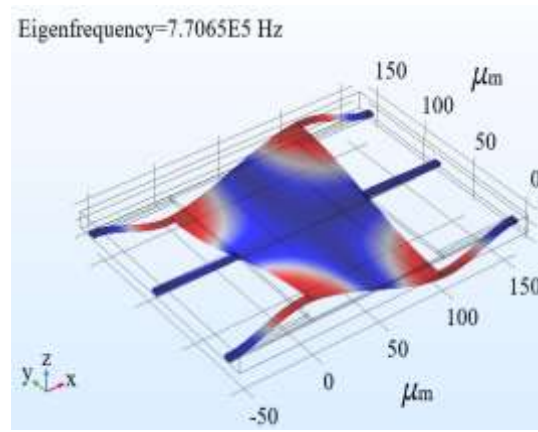
Mode-III



Mode-IV



Mode-V



Mode-VI

Table 6. shows the stress distribution and different modes of vibrations. For stress analysis we used linear elastic, homogeneous and isotropic properties of the materials. We considered three dimensional problems by applying the conditions of elastic stretching and compression in perpendicular directions for the displacement of structure. We applied boundary conditions for the approximate solution of the device was obtained from the general set of simulations. The values of stress and displacement were calculated by using a particular set of simulations.

Color bars denotes the lesser and greater values of stresses created in the device. Von Mises stress is a value used to define material yield or failure. This study is generally used for alloys and ductile materials, for example metals. The von Mises give in standard conditions that if the von Mises stress of a material below consignment is different or superior than the yield border of the alike objects under effortless tension, then the material will yield. The membrane under loading effect is displaced due to stress-strain relation. The stress is produced due to external force and membrane is displaced due to deformation produced by the strain. This relation represents property of the material that composes the body.

Table 6. Stress distribution in the structure of switch with respect to six modes

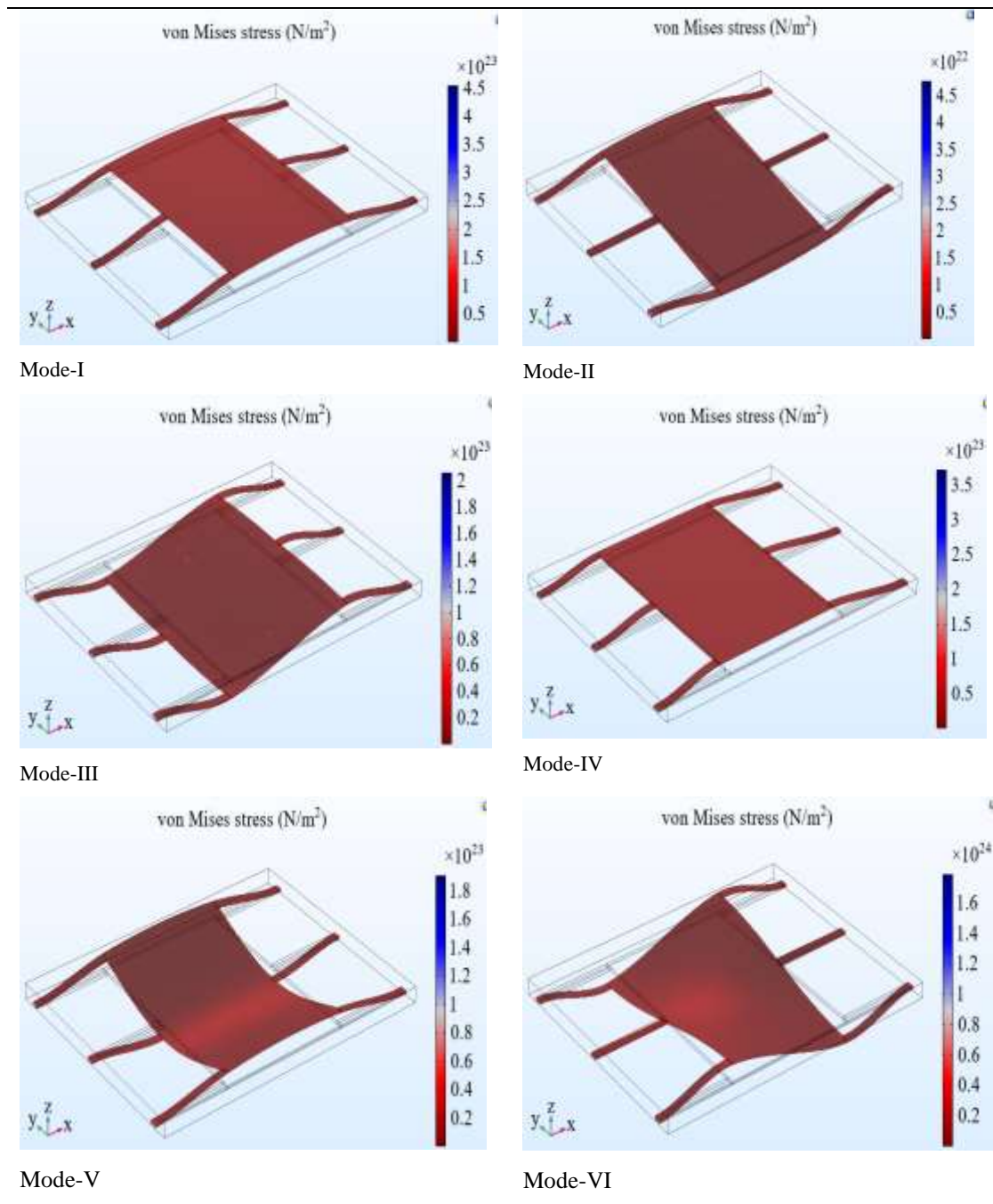


Figure 23 describes the displacement of the cantilever due to applied biased voltage. The design parameters are same as used for SiN_3 based device. The displacement of $0.9\mu\text{m}$ is produced when the biased voltage is reached to 10V.

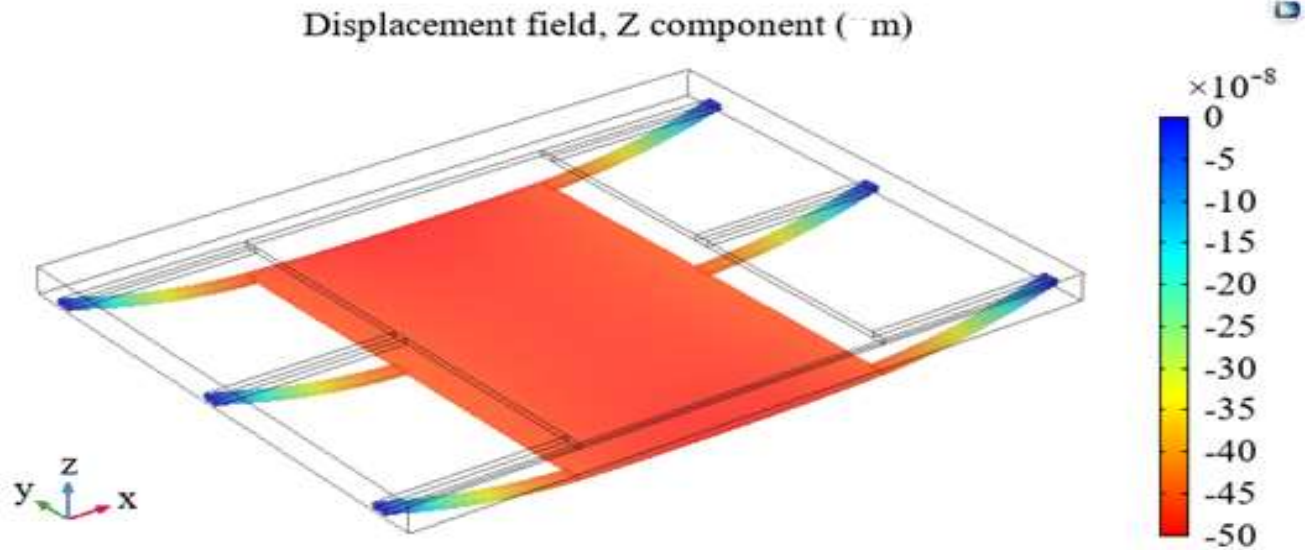


Figure 24. Maximum displacements due to biased voltage

3D graph shown in figure 25. demonstrates the distribution of electrical potential produced due to the biased voltage. The red color shows the higher potential and small arrows shows the electric field.

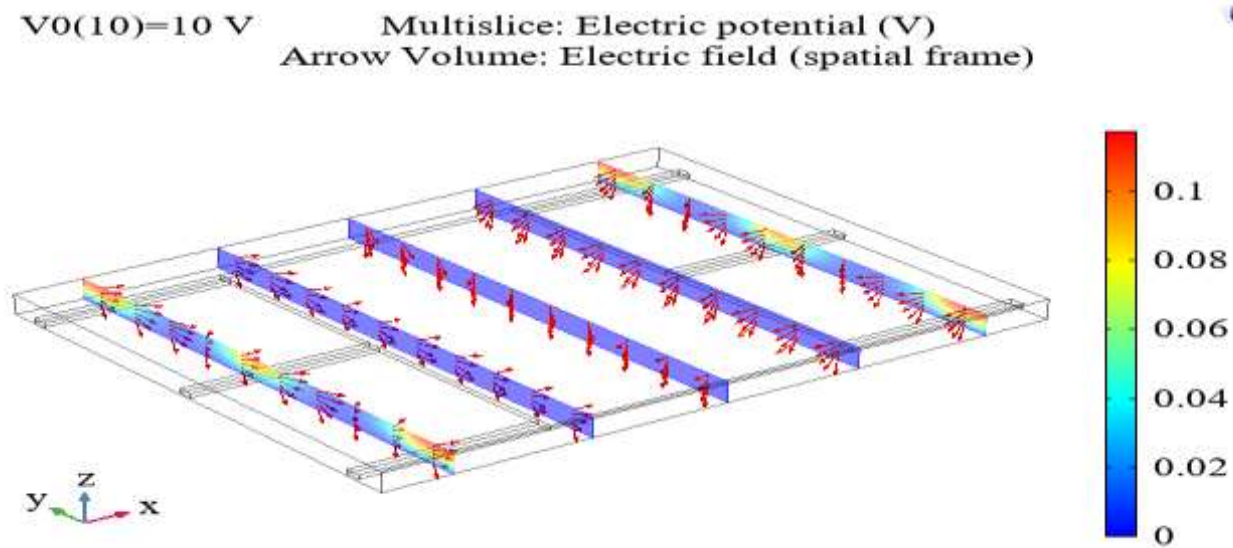


Figure 25. The response of the device in terms of electrical potential

Figures 26. represent the shapes of plate displacement as a function of arc length. Figure presents the impact of biased voltages on the pull-in displacement. We noticed that when the

voltage is increase up to 10V, the pull-in force is increased which causes in producing large displacement $0.9\mu\text{m}$ which is the limit of plate collapsing with the grounded electrode.

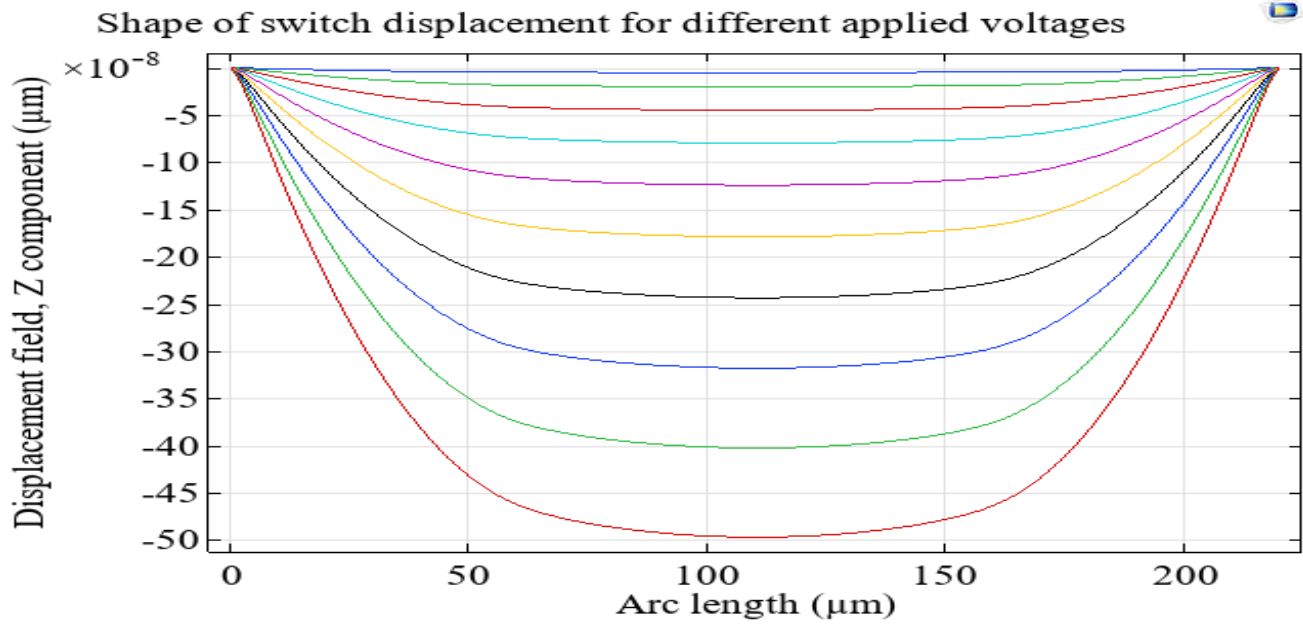


Figure 26. Pull-in displacement due to biased voltage

Figure 27 illustrate the impacts of voltage on the maximum displacement of the device. We observed that when the biased voltage is improved from 1V to 10V, the displacement along z-axis is also increased to $0.85\mu\text{m}$.

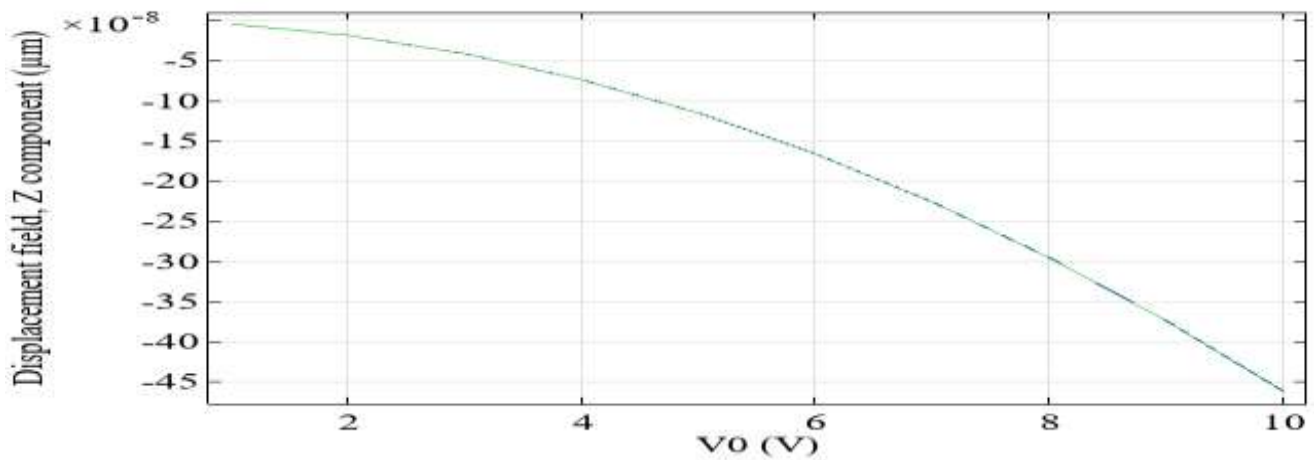


Figure 27. Relations between voltage and displacement

Figure 28 shows the line graph of increasing capacitance with respect to biased voltage. We observed that at higher voltage 10V, the capacitance of the device is also increased.

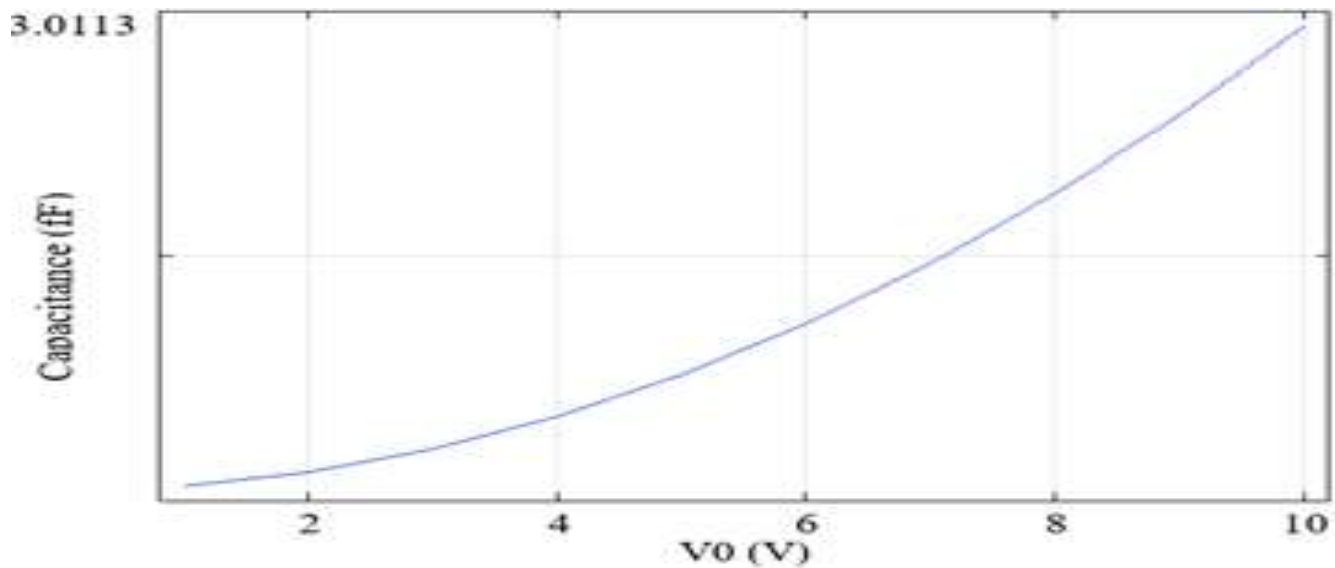


Figure 28. Effect of biased voltage on the capacitance

Analysis of Performance Parameters of SiO₂ based Switch

This section investigates the behavior of device in terms of modes and stresses. The dynamic characteristics of devices are intensely depending on electric and mechanical elements, material properties and their geometry. There is mutual relation among electric and mechanical dynamics in the device. Therefore, for virtual prototyping, finite element modeling and simulation is considered as more efficient designing approach for electrostatic devices. Table 7 shows six different modes of vibration under Eigen frequencies. The change in Eigen frequency caused a change in mode shape.

Table 7. Eigen frequency and mode shapes of MEMS based switch

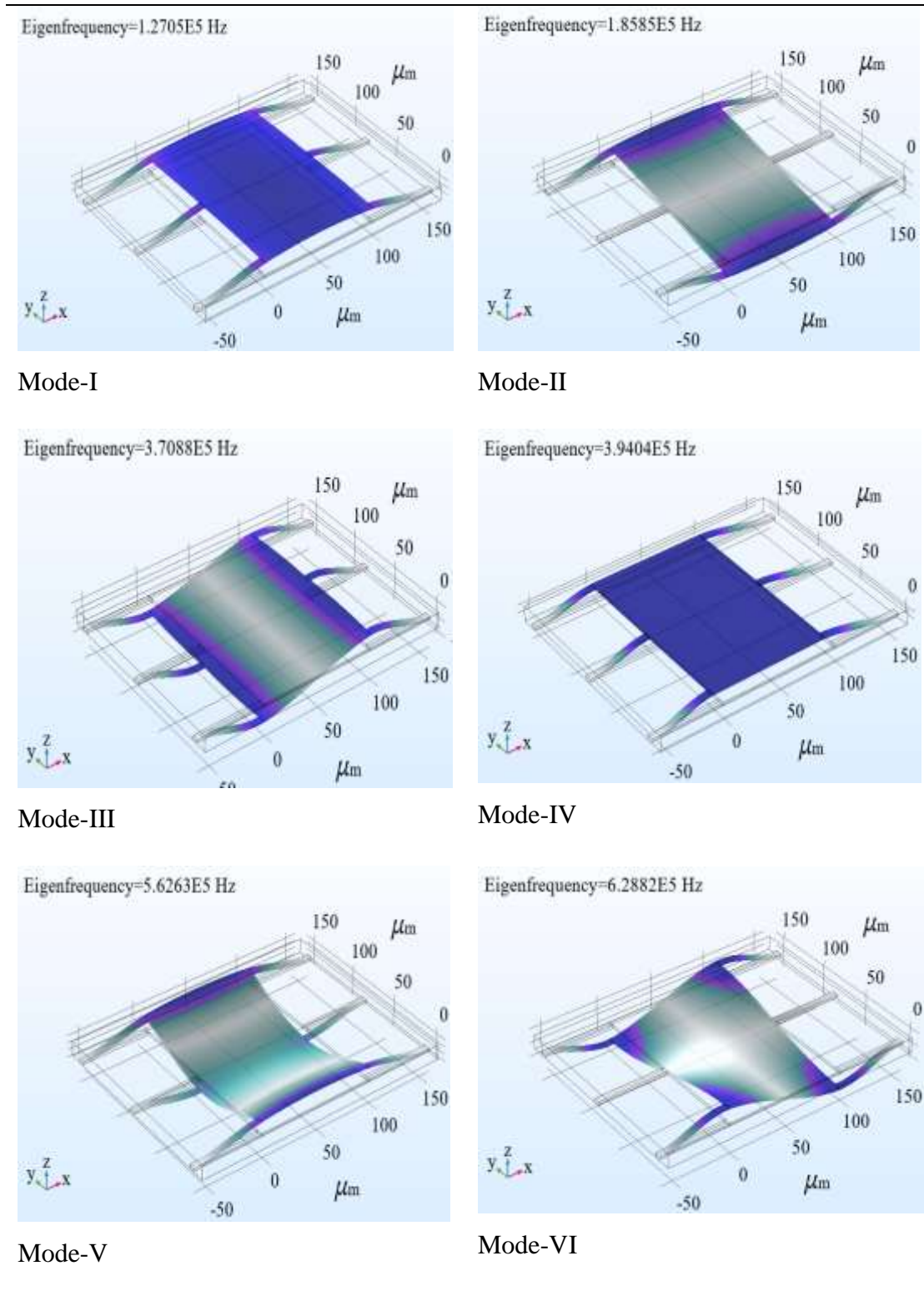


Table 8. shows the stress distribution and different modes of vibrations. For stress analysis we used linear elastic, homogeneous and isotropic properties of the materials. We considered three dimensional problems by applying the conditions of elastic stretching and compression in perpendicular directions for the displacement of structure. We applied boundary conditions for the approximate solution of the device was obtained from the general set of simulations. The values of stress and displacement were calculated by using a particular set of simulations.

Table 8. Stress distribution in the structure of switch with respect to six modes

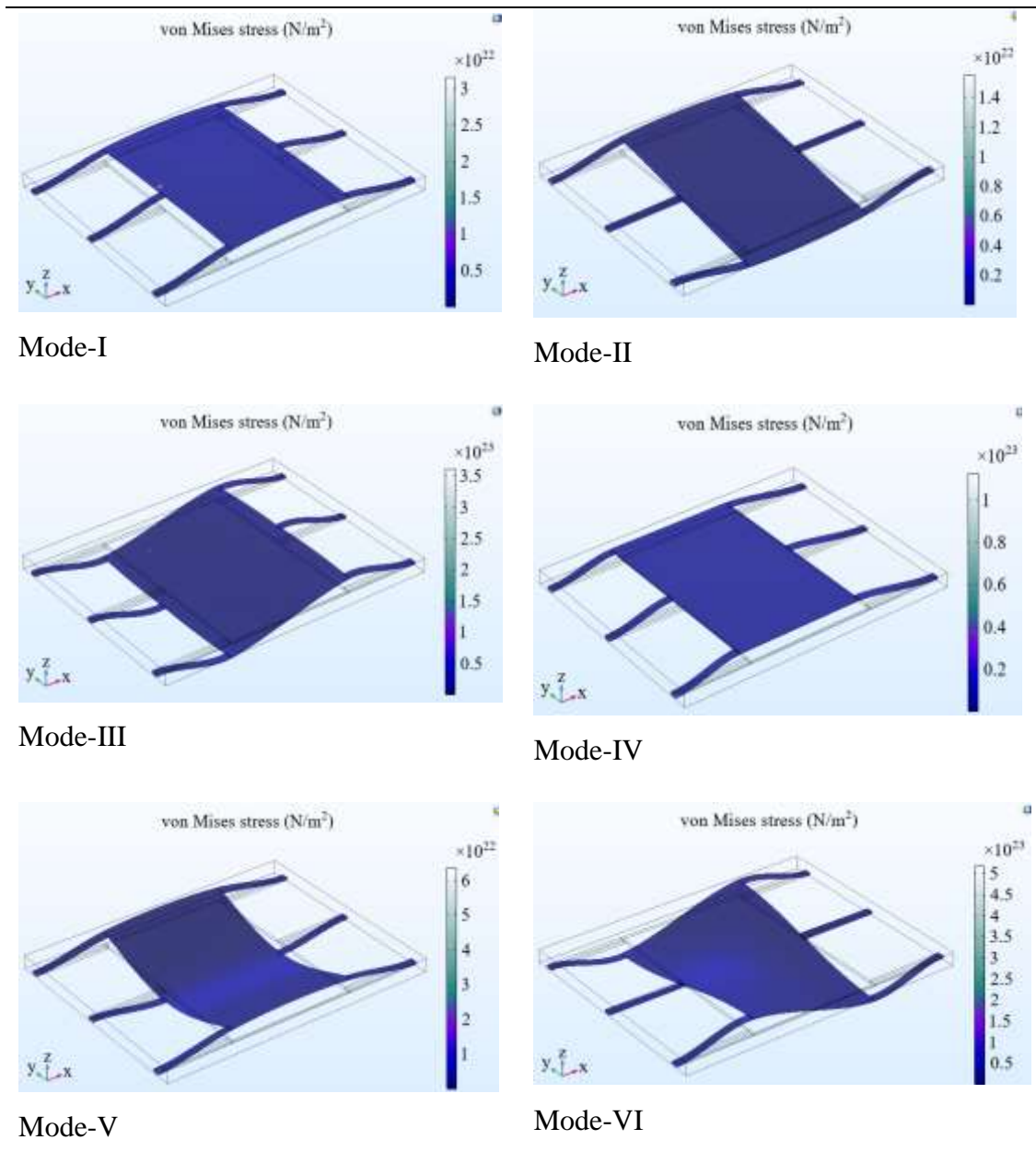


Figure 29 shows the layout of displacement field and mesh displacement of the plate at 10V. As the voltage is improved from 1 to 10 V, the displacement is generated due to the pull-in force. Figure 30 shows the electric potential allotment. At the slices of plate the arrows show the electric field is perpendicular in the middle of the plate. We observed the electric potential of 0.08V

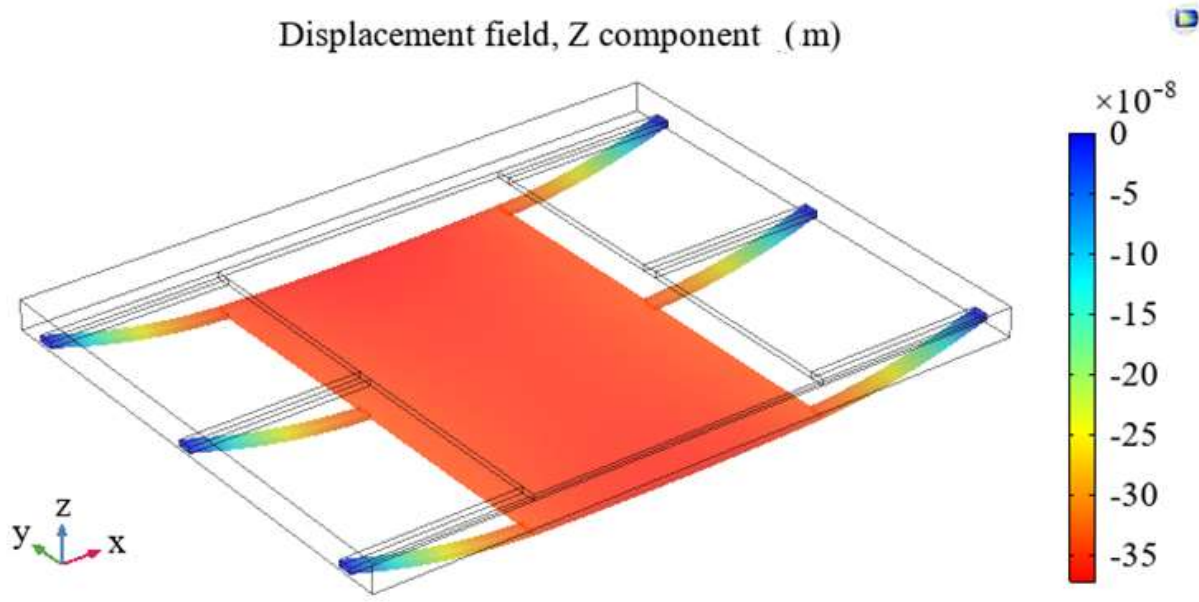


Figure 29 Change in displacement due to applied voltage

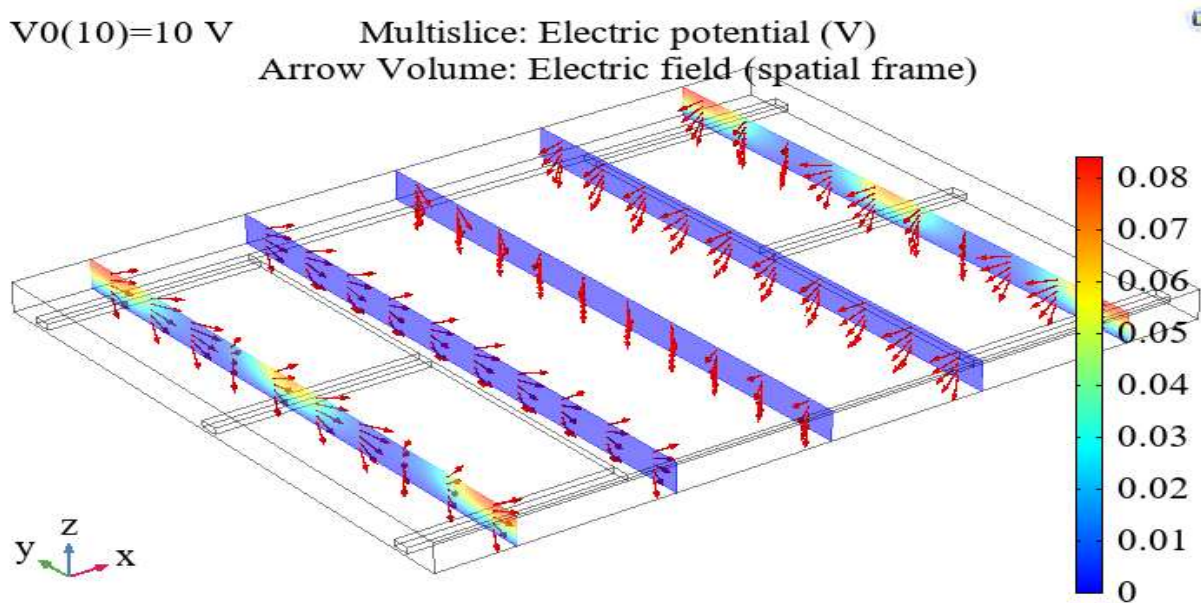


Figure 30. Distribution of electrical potential and electric field

Figure 31. shows the shapes of deflections of FEM based switch at different voltages. Figure 17. demonstrate the line graph of maximum displacement of the plate as meaning of functional voltage. The limitation of biased voltage is considered while designing electrostatic devices, since soaring voltage yields great electrostatic force that can be the reason of device failure due to stiction of plate to the grounded electrode. Moreover higher voltage may be the cause of inducing the pull-in effect owing to huge capacitance resulting in a non-symmetrical actuation.

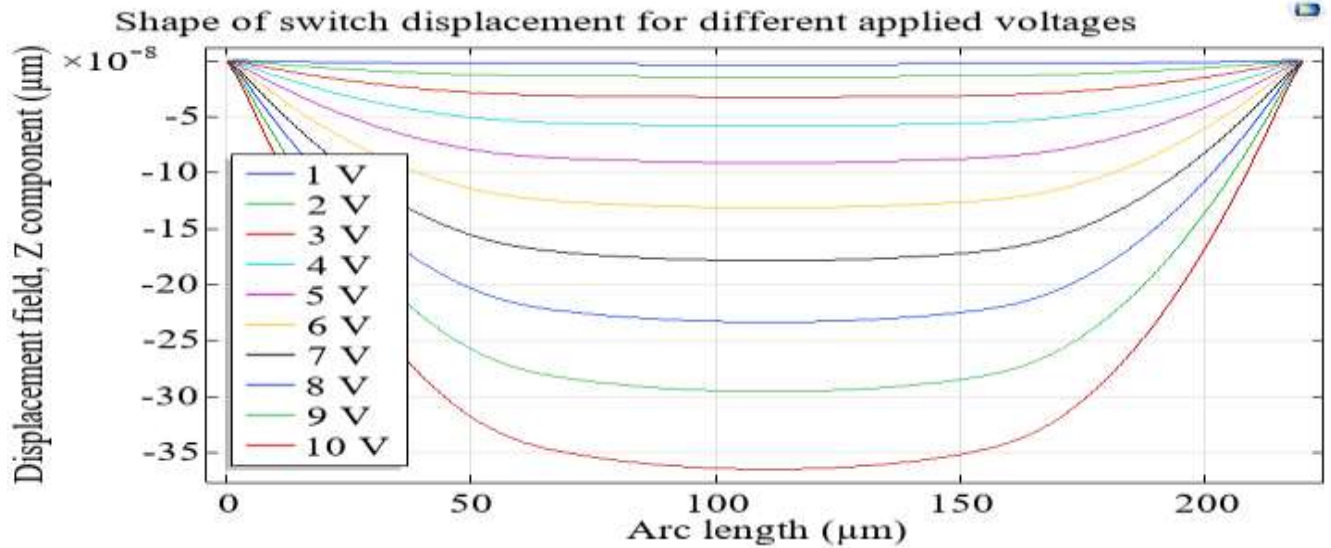


Figure 31. Pull-in displacement due to biased voltage

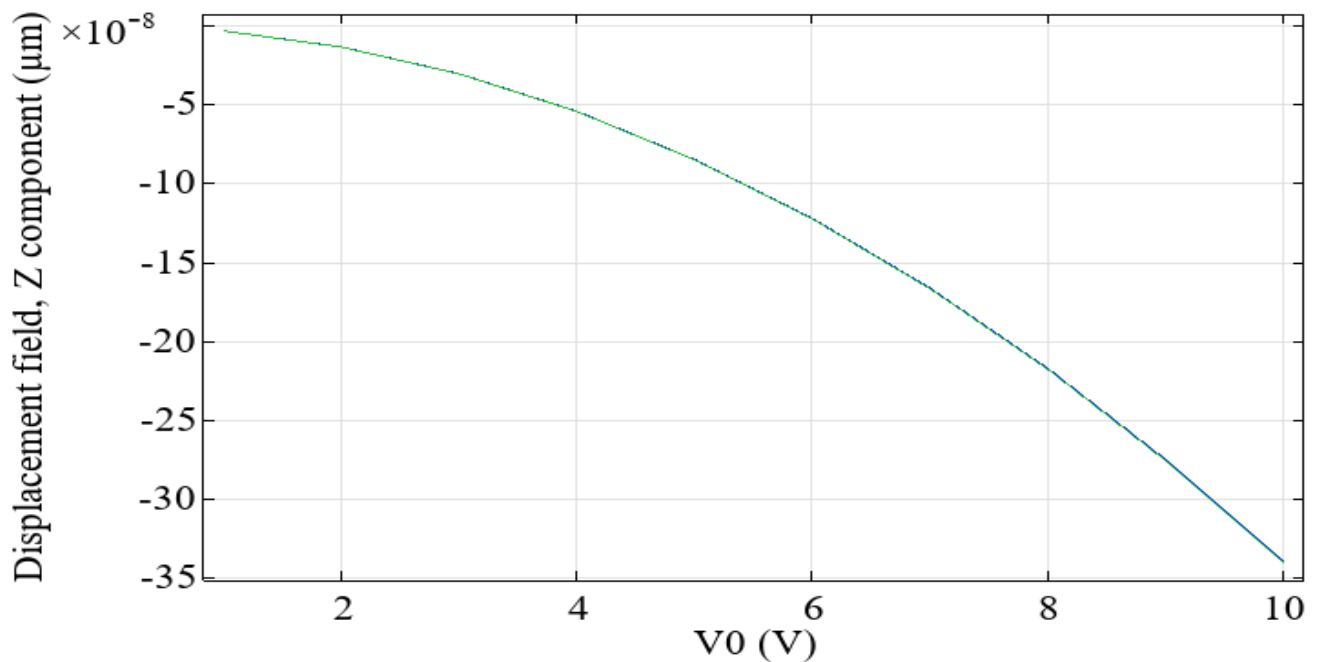


Figure 32. Displacement of plate as function of voltage

Figure 33 represents that capacitance of switch also dependent on the applied voltage. In order to avoid the stiction of plate we use bias voltage of 10V during stationary analysis. The line graph shows that the capacitance is increased by higher applied voltage.

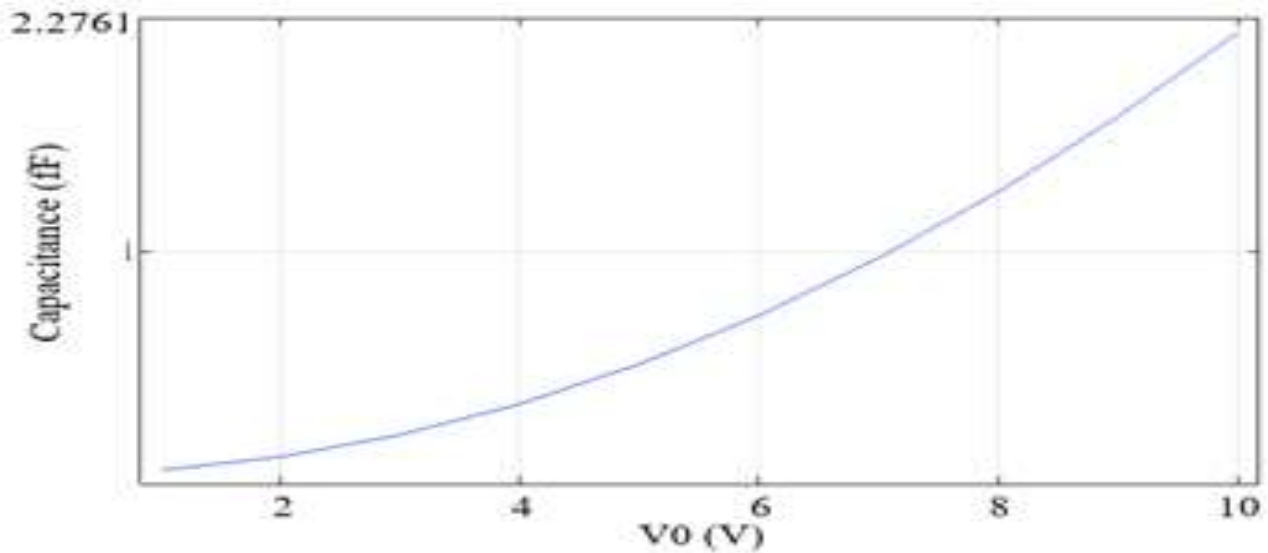


Figure 33. Effect of voltage on the capacitance of the switch

Comparison between Si, SiO₂ and SiN₃ based Switches

Efficiency analysis of the proposed devices was performed by comparing the performance parameters of single crystal Silicon, SiO₂ and SiN₃ based MEMS switches as shown in Table 9. The output response of all three devices was investigated using DC voltage 10V. We observed that measured values of performance parameters of single crystal Silicon based device are higher as compared to SiO₂ and SiN₃ based devices under same boundary conditions and design parameters. We concluded that Si material is significant for better results in switching application. Si material has higher electrical and capacitive response as compared to the other two materials.

Table 9. Comparison between performance parameters of MEMS switches

Material	Displacement (μm)	Electrical (V)	Potential	Capacitance (pF)
Si single crystal	0.8	0.14		3.5833
SiN ₃	0.5	0.12		3.0113
SiO ₂	0.35	0.08		2.2761

CONCLUSION

The main objective of this research was to study the Designing and Simulation of Electrostatic MEMS Switch in COMSOL Multi physics. The goal was to improve the existing MEMS electrostatic switches. As the higher consumption of power is the main issue in various devices, so, the basic aim of this research is to achieve RF MEMS switches along with less actuation voltage.

A comparison between the three materials like single crystal Silicon (Si), Silicon Dioxide (SiO_2) and Silicon Nitride (SiN_3) based MEMS Switches have been made. As per analysis of the results we conclude that Si material is significant for better results in switching application because values of performance parameters of single crystal Silicon based device are higher as compared to SiO_2 and SiN_3 based devices under same boundary conditions. Si material has higher electrical and capacitive response as compared to other two materials.

REFERENCES

1. Sawane M, Prasad M. MEMS piezoelectric sensor for self-powered devices: A review. *Materials Science in Semiconductor Processing*. 2023;158:107324.
2. Ali WR, Prasad M. Piezoelectric MEMS based acoustic sensors: A review. *Sensors and Actuators A: Physical*. 2020;301:111756.
3. Verma G, Mondal K, Gupta A. Si-based MEMS resonant sensor: A review from microfabrication perspective. *Microelectronics Journal*. 2021;118:105210.
4. Faudzi AAM, Sabzehmeidani Y, Suzumori K. Application of micro-electro-mechanical systems (MEMS) as sensors: A review. *Journal of Robotics and Mechatronics*. 2020;32(2):281-8.
5. Kurmendra, Kumar R. A review on RF micro-electro-mechanical-systems (MEMS) switch for radio frequency applications. *Microsystem Technologies*. 2021;27(7):2525-42.
6. Percy JJ, Kanthamani S. Revolutionizing wireless communication: a review perspective on design and optimization of RF MEMS switches. *Microelectronics Journal*. 2023:105891.
7. Cao T, Hu T, Zhao Y. Research status and development trend of MEMS switches: A review. *Micromachines*. 2020;11(7):694.
8. Mirza A, Hamid NH, Md Khir MH, Ashraf K, Jan M, Riaz K. Design, Modeling and Simulation of CMOS-MEMS Piezoresistive Cantilever Based Carbon Dioxide Gas Sensor for Capnometry. *Advanced Materials Research*. 2012;403:3769-74.
9. Mirza A, Arshad FB. Performance analysis of cyclostationary sensing in cognitive radio networks. 2011.
10. Atik AC, Özkan MD, Özgür E, KÜlah H, Yıldırım E. Modeling and fabrication of electrostatically actuated diaphragms for on-chip valving of MEMS-compatible microfluidic systems. *Journal of Micromechanics and Microengineering*. 2020;30(11):115001.

11. Chae U, Yu H-Y, Lee C, Cho I-J. A hybrid RF MEMS switch actuated by the combination of bidirectional thermal actuations and electrostatic holding. IEEE Transactions on Microwave Theory and Techniques. 2020;68(8):3461-70.
12. Chokkara SP, Gaur A, Sravani KG, Balaji B, Rao KS. Design, simulation and analysis of a slotted RF MEMS switch. Transactions on Electrical and Electronic Materials. 2022:1-11.
13. Shanthi G, Rao KS, Sravani KG. Performance analysis of EBG bandstop filter using U: shaped meander type electrostatically actuated RF MEMS switch. Microsystem Technologies. 2021;27(10):3743-50.
14. Mousavi M, Alzgoool M, Towfighian S. Electrostatic levitation: an elegant method to control MEMS switching operation. Nonlinear Dynamics. 2021;104(4):3139-55.
15. Mirza A, Khir MHM, Dennis JO, Ashraf K, Hamid NH, editors. Design, modeling and simulation of CMOS MEMS cantilever for carbon dioxide gas sensing. 2011 IEEE Regional Symposium on Micro and Nano Electronics; 2011: IEEE.